ČESKÁ ZEMĚDĚLSKÁ UNIVERZITA V PRAZE

(Czech University of Life Sciences Prague)

FAKULTA ŽIVOTNÍHO PROSTŘEDÍ

(Faculty of Environmental Sciences)

The use of nano zero-valent iron (nZVI) in soil remediation and its interactions with plants

Diploma Thesis

Supervisor: Ing. Zuzana Vaňková, Ph.D.

2023/2024 **Mayda Rojnik**

CZECH UNIVERSITY OF LIFE SCIENCES PRAGUE

Faculty of Environmental Sciences

DIPLOMA THESIS ASSIGNMENT

Bc. Mayda Rojnik

Environmental Geosciences

Thesis title

The use of nano zerovant iron (nZVI) in soil remediation and its interactions with plants

---

Objectives of thesis

The aim of the first part of the thesis is to provide an overview of the main findings concerning the use of nano zerovalent particles (nZVI) for the remediation of contaminated soils. Its basic properties and ways of synthesis will be summarized, along with information on nZVI´s application in soil remediation, environmental fate and influence on plants.

In the experimental part of the thesis, sulfidated nZVI (S-nZVI) with/without the addition of thermally treated sewage sludge will be mixed into soil contaminated by the smelting industry, and two grass species (Arrhenatherum elatius and Festuca rubra) will be grown on amended soils. The influence of applied amendments on the solubility of the main metallic contaminants will be determined using water extraction, and the effects on plants will be evaluated based on plant height, biomass and content of metals/metalloids.

Methodology

1. The review part is based on verified literature sources, mainly articles in scientific journals.

2. A greenhouse experiment followed by laboratory analyses will be performed. Two grass species will be grown in contaminated soil amended by S-nZVI and/or thermally stabilized sewage sludge. After the harvest, the solubility of the main metallic contaminants will be determined using water extraction, and the effects on plants will be evaluated based on plant height, biomass and content of metals/metalloids.

3. The resulting data will be processed and evaluated. The results will be discussed, and clearly formulated conclusions will be drawn.

The proposed extent of the thesis

approximately 60 pages as needed

Keywords

immobilization, metals, metalloids, extraction, biomass

Recommended information sources

Alazaiza, M. Y. D., Albahnasawi, A., Copty, N. K., Bashir, M. J. K., Nassani, D. E., Maskari, T. A., Amr, S. S. A., Abujazar, M. S. S., 2022: Nanoscale Zero-Valent Iron Application for the Treatment of Soil, Wastewater and Groundwater Contaminated with Heavy Metals: A Review. Desalination and Water Treatment, volume 253: 194–210.

Ali, H., Khan, E., Ilahi, I., 2019: Environmental Chemistry and Ecotoxicology of Hazardous Heavy Metals: Environmental Persistence, Toxicity, and Bioaccumulation. Journal of Chemistry, volume 2019: 6730305.

Cui, X., Hou, D., Tang, Y., Liu, M., Qie, H., Qian, T., Xu, R., Lin, A., Xu, X., 2023: Effects of The Application of Nanoscale Zero-Valent Iron on Plants: Meta Analysis, Mechanism, And Prospects. Science of The Total Environment, volume 900: 165873.

Garcia, A. N., Zhang, Y., Ghoshal, S., He, F., O´Carroll, D. M., 2021: Recent Advances in Sulphidated Zerovalent Iron for Contaminant Transformation. Environmental Science & Technology, volume 55, issue 13: 8464-8483.

Guo, Y., Li, X., Liang, L., Lin, Z., Su, X., Zhang, W., 2021: Immobilization of Cadmium in Contaminated Soils Using Sulphidated Nanoscale Zero-Valent Iron: Effectiveness and Remediation Mechanism. Journal of Hazardous Materials, volume 420: 126605.

Latif, A., Sheng, D., Sun, K., Si, Y., Azeem, M., Abbas, A., Bilal, M., 2020: Remediation of Heavy Metals Polluted Environment Using Fe-Based Nanoparticles: Mechanisms, Influencing Factors, And Environmental Implications. Environmental Pollution, volume 264: 114728.

Li, M., Zhang, P., Adeel, M., Guo, Z., Chetwynd, A. J., Ma, C., Bai, T., Hao, Y., Rui, Y., 2021a: Physiological Impacts of Zero Valent Iron, Fe3O4 and Fe2O3 Nanoparticles in Rice Plants and Their Potential as Fe Fertilizers. Environmental Pollution, volume 269: 116134.

Ma, X., Gurung, A., Deng, Y., 2013: Phytotoxicity and Uptake of Nanoscale Zero-Valent Iron (nZVI) by Two Plant Species. Science of the Total Environment, volume 443: 844-849.

Expected date of thesis defence
2023/24 SS – FES

The Diploma Thesis Supervisor
Ing. Zuzana Vaňková, Ph.D.

Supervising department
Department of Environmental Geosciences

Advisor of thesis
Omolola Elizabeth Ojo

Electronic approval: 27. 3. 2024
prof. RNDr. Vladislav Chrastný, Ph.D.
Head of department

Electronic approval: 27. 3. 2024
prof. RNDr. Michael Komárek, Ph.D.
Dean

Prague on 27. 03. 2024

Author´s statement

I hereby declare that I have independently elaborated the diploma/final thesis with the topic of: "The use of nano zero-valent iron (nZVI) in soil remediation and its interactions with plants" and that I have cited all the information sources that I used in the thesis and that are also listed at the end of the thesis in the list of used information sources.

I am aware that my diploma/final thesis is subject to Act No. 121/2000 Coll., on copyright, on rights related to copyright and on amendment of some acts, as amended by later regulations, particularly the provisions of Section 35(3) of the act on the use of the thesis.

I am aware that by submitting the diploma/final thesis I agree with its publication under Act No. 111/1998 Coll., on universities and on the change and amendments of some acts, as amended, regardless of the result of its defence.

With my own signature, I also declare that the electronic version is identical to the printed version and the data stated in the thesis has been processed in relation to the GDPR.

In....., date.....

.....

Acknowledgments

I would like to express my gratitude to my consultant Omolola Elizabeth Ojo for her guidance and assistance throughout this research endeavour with which I expanded my knowledge and understanding of the experimental work and the topic itself. Special thanks also go to my supervisor Ing. Zuzana Vaňková, Ph.D., for her insightful feedback, recommendations, and mentorship which helped me shape the quality of this thesis and motivate me. To my family, especially my parents Nives and Raymond, friends, Antonija and Tin, whose patience, encouragement, and support were the grounds of this work. And my partner, Zachary, who I am deeply grateful for the love and encouragement during this whole academic journey.

Abstract

Key words: immobilization, metals, metalloids, extraction, biomass

As soil contamination still remains to be one of the universal environmental obstacles, necessities for innovative remediation solution such as nZVI are in dire need. This thesis will therefore explore the use of nZVI in soil remediation and its behaviours in relation to two plant species *Arrhenatherum elatius* and *Festuca rubra*. Overview of nZVI's properties and applications, followed by an experimental part which will delve more in depth and analyse the efficiency of sulphiated nZVI and thermally treated sludge in hopes to find synergy among them for remediation purposes of the highly contaminated Technosol.

The literary research will define nZVI and how it developed throughout the years based on the research directions that branched out following the specificities of remediation. Successful and unsuccessful remediation findings of nZVI, especially considering potentially risky elements, while also bringing to light its potential toxicity, alongside its other challenges and limitations, will be critically discussed. As this thesis also regards interactions with plants, supported phytoremediation and phytotoxicity will be explored as well. The critical review on the properties of nZVI can point out and identify future research gaps that need to be investigated.

Likewise, the experimental part will analyse and discuss the complexities behind this innovative remediation technique and bring more future insight in this more sustainable way of soil remediation through methods of aqua regia, soil water extraction, total elemental concentrations, pH determination, and plant biomass and digestion. The experimental findings will be discussed based on the results which showed effective synergy between nZVI and sludge via their successfulness in simultaneously immobilizing contaminants while also providing essential nutrients.

Table Of Contents

1 Introduction

World´s universal environmental challenge is soil contamination, and as Hugh Hammond Bennett once said, "Take care of the land, and the land will take care of you" (1947). If we, as a part of the same ecosystem, do not find remediation techniques as solution to our own polluting consequences, our wellbeing and health will be disrupted. Throughout the years many remediation techniques emerged, but they are sometimes falling short in the realm of complexity and scale of remediation required. Therefore, new innovative solutions have been emerging and one of them is the promising nano zero-valent iron (nZVI), which this Master thesis will explore.

The thesis will overview nZVIs properties, short history, and introduce the mining town of Příbram, where the soil was taken from for the experimental part of this thesis. The investigation of how to reach the full potential of nZVI through synthesis and modification techniques will be overviewed, and sulphidated nZVI used in the experimental part will be introduced. The importance of synthesis lays in the specificity of remediation needs in research. With the fundamentals of synthesis, application examples of nZVI will follow. Successful S-nZVI remediation studies, which deal with potentially risky metals and the simultaneous interactions with soil properties and constituents, will be discussed. To understand the success of using nZVI, the reactivity mechanisms during remediation, followed by nZVI environmental fate, will be covered. After the exploration of interactions between nZVI and soil, interactions between nZVI and plants will be overviewed, as both are interconnected. It will cover potential phytotoxicity and potential cooperation between nZVI and plants in remediation strategies. Even though there are great positives of nZVI in remediation, it is important to review its limitations and challenges. Continuing the critical review, nZVI remediation will be compared with other alternative remediation strategies and techniques. Lastly, the gaps in research will be explored to direct the research and discourse in the future, regarding the use of nZVI.

The literature review will contribute to a better background and understanding of the experiment, which dealt with the use of S-nZVI and its interaction and relation with *Festuca rubra* and *Arrhenatherum elatius* plants in the remediation of Příbram soil. The chemical and physical analysis and characterisation will unravel the complex remediation influence that nZVI poses to plant growth and soil parameters.

2 Objectives of the Thesis

The aim of the first part of the thesis is to provide an overview of the main findings concerning the use of nano zerovalent particles (nZVI) for the remediation of contaminated soils. Its basic properties and ways of synthesis will be summarized, along with information on nZVI´s application in soil remediation, environmental fate and influence on plants.

In the experimental part of the thesis, sulphidated nZVI (S-nZVI) with/without the addition of thermally treated sewage sludge will be mixed into soil contaminated by the smelting industry, and two grass species (*Arrhenatherum elatius* and *Festuca rubra*) will be grown on amended soils. The influence of applied amendments on the solubility of the main metallic contaminants will be determined using water extraction, and the effects on plants will be evaluated based on plant height, biomass and content of metals/metalloids.

3 Literary Research

3.1 Introduction to Nano Zero-valent Iron (nZVI) in Soil Remediation:

3.1.1 Defining nZVI and its properties

The nZVI is a nanoparticle consisting of a zero-valent iron core, which acts as an electron donor and main contributor of reductivity, and an iron oxide structure that encapsulates the core, and consequently shells it. Its importance in the environmental context comes from its versatility and the fact that it is easily synthesized and modified; the element from which it is made, iron, is abundant, cheap, and easily available in the environment (Mu et al., 2017). nZVI´s main properties relevant to soil remediation are magnetic properties, aggregation tendencies (Eljamal et al., 2020), transportability (Liang et al., 2014), biocompatibility (Nadagouda et al., 2010), and nZVI´s most important property – size. nZVI´s size is less than 100 nm in its diameter and because of that, it adds to another important property, high surface area per unit mass. The nano size property contributes to increased reactivity, effectiveness in various types of environments in terms of transportability, and more chemical reaction sites on its surface, such as reduction, catalysis and adsorption (Mu et al., 2017).

The iron oxide shell structure, alongside nZVI's high surface area, is the most important part of the nZVI particle because its electrostatic interactions allow the solute to adsorb and direct the transfer of electrons with the core. Due to its complex surface composition, it conducts the chemical processes leading to environmental contaminants removal processes (Mu et al., 2017), such as oxidation, adsorption and precipitation or co-precipitation (MacKenzie & Georgi, 2019).

The study findings observed by Ling et al. (2017) regarding the nZVI´s iron oxide shell and zero-valent core suggest that the brightness and thickness differences are what separate the two. Therefore, the "high-angle dark-field (HAADF)" imaging is also used to show potentially risky metal regions on the nZVI particle based on the particle thickness and atomic number differences. The zero-valent core like the shell shows up as bright intense, oxygen sparse, unlike the dim, oxygen full area of the 50-100 nm particle deducted via iron-oxygen overlaying. The atomic ratio mapping of the shell also shows that the stoichiometry of the outer shell part is close to one of iron oxyhydroxide and of the inner shell to one of ferric oxide and ferrous oxide, proving the oxide shelling of the core. The zero-valent iron core, which, on the other hand, by

the line profiling via XEDS iron counts shows up deeper and darker towards the centre of the particle showcasing higher iron density area.

In the critical review article by Mu et al. (2017), they specifically interpret the properties of the oxide shell of the nZVI and its remediation aspects. They state that by reviewing the transmission electron microscopy (TEM) images, it is possible to see a 2 nm thick membrane of a grey colour which is the shell, as previously mentioned, composed of iron oxides, produced through the corrosion by oxygen or water of the iron core. If nZVI is synthesized in a water medium, the core is oxidized by water or oxygen, but if synthesized in a solvent-free environment, it is oxidized rapidly by air. Therefore, the type of oxide shell produced depends on the synthesis media and its laboratory and storage conditions (MacKenzie & Georgi, 2019).

Except for TEM, for the characterization of the shell, Mu et al. (2017) also reviewed that the use of diffractometric and spectroscopic analyses is useful in portraying its crystalline structure, elements present, phases, redox states, etc. The porous shell of nZVI allows the passage of pollutants, mostly of an organic nature, to the reductive iron core through concentration gradients. If the conditions for that are not met, the pollutants can also be reduced in the shell, which is better in the thermodynamic sense with the electrons donated from the iron core to reduce pollutants. But if this interaction is prolonged, it can thicken the shell by which the porosity would be decreased, and inhibition increased of the transfer of electrons and pollutants and their interactions.

On the other hand, the removal of inorganic pollutants mechanism, such as potentially risky metals and their ions, is determined by redox potential. If the potentially risky metal ion redox potential is higher than that of one of the iron cores, then they are reduced to their lower valence states or removed by sorption with the products of the iron core corrosion. But, if the redox potential is lower than the redox potential of the iron core, they are removed either by a redox reaction, co-precipitation or adsorption on the shell (Tarekegn et al., 2021).

To improve the stability and performance of the shells´ pollutant removal, modifiers are often used, such as vacuum annealing (Crane & Scott, 2013), depassivation (Xie & Cwiertny, 2010) or polymer coating, which allows the nanoparticles not to agglomerate due to their magnetic and van der Waals forces, and

improve the sense of specific surface area and their reactivity with the pollutants (Mokete et al., 2020). Even with all this information on the oxide shell of the nZVI, the authors acknowledge that there is still much to be discovered in the understanding of the complex mechanisms responsible for pollutant removal (Mu et al., 2017).

3.1.2 Historical development of nZVI use in soil remediation

The history of nZVI dates back to the 60s when it was first synthesized from iron salts using borohydride reduction but not until 1997 when it was first synthesized by researchers Wang and Zhang specifically for environmental remediation (Phenrat et al., 2019; Wang & Zhang, 1997). Due to nZVI´s small size and great reductive properties, it brings attention to researchers as a way to avoid limitations of other technologies used in environmental remediation, such as low degradation per mass of the agents used for remediation (Phenrat et al., 2019).

In the early 2000s, nZVI research finally reached field applications, such as the first field assessment by Elliot and Zhang in 2001, which showed that bare unmodified nZVI is not efficient enough to be used as an agent alone (Elliot & Zhang, 2001). The first field assessment using nZVI for the removal of As was performed by Kanel et al. (2005), Dense Nonaqueous Phase Liquids (DNAPL) treatment using nZVI by Taghavy et al. (2010) and chlorinated volatile organic compounds (cVOCs) biodegradation remediation by Xiu et al. (2010). Alongside the field applications, properties of nZVI were researched, such as correlativity of nZVI and dichlorination by Nurmi et al. (2005) and Liu et al. (2005), promotion of aggregation by magnetism by Phenrat et al. (2007) and Saleh et al. (2008) investigated the sticking coefficient of nZVI. In 2004, the researchers shifted the investigation towards the improvement of nZVI as a remediation agent with a focus on its mobility and deliverability (Schrick et al., 2004). By the end of the 2000s, the investigations also turned towards its toxicity. Since no data was available on that topic and many other nanoparticles were being investigated at the same time because of their increasing use in day-to-day commercial products, nZVI had to be tested too (Phenrat et al., 2019). So, in 2008, Lee et al. (2008) made the first ecotoxicological test, and in 2009, Phenrat et al. (2009b) performed the first toxicological test of nZVI. Following the toxicity research, there was also a risk and benefits assessment of nZVI in 2010 by Grieger et al. (2010). In the 2010s, the

research went more in the direction of experimenting with nZVI modifications with other materials, such as the first nZVI with a foam base by Ding et al. (2013), followed by the first sulphidated nZVI by Fan et al. (2013), and many more modifiers such as carbon or different polymers became popular in research due to interest in improving nZVIs transport and agglomerabillity (Phenrat et al., 2019). Alongside modifications, different predictive models were investigated due to the fact that nZVI can be effective only if it has specific location delivery, starting with the first model predicting the transport of nZVI in a porous environment by Phenrat et al. (2010), model of transport on a field scale of carboxymethyl cellulose modified nZVI by Krol et al. (2013), and the first tool based on Modular three-dimensional finite-difference ground-water flow model (MODFLOW) for the transport of nZVI modified with polymers by Babakhani et al. (2015). Besides all of these mentioned research papers, the number of remediated sites using nZVI as a remediation agent reached 77 in 2017 in countries of Europe, Canada, the USA and Taiwan (Phenrat et al., 2019).

More specifically, in Europe, NanoRem has been the leading project from 2013 to 2018 in investigating the use of nanotechnological remediation in end-user utilization based on research on a laboratory scale (NanoRem, 2023). It was funded by the European Commission from the European Union Seventh Framework Programme (Decision No. 1982/2006/EC). NanoRem´s main aims were lowering production costs of nanomaterials on a commercial scale, finding the right nanoparticles for practical use, comprehensive models of application, sharing information with key stakeholders interested in nanoparticle remediation, and reviewing the performance, cost, and fate from field assessments performed (NanoRem, 2023).

3.2 Synthesis Techniques for nZVI:

3.2.1 Basic principles and types of nZVI synthesis

When classifying the nZVI synthesis techniques, it is common to differentiate between two methods, top-down and bottom-up. Categorizing based on the process type further separates them into chemical, physical or green methods (MacKenzie & Georgi, 2019).

The physical process type of synthesis is oftentimes associated with top-down techniques such as lithography, grinding, and milling, with the action of mechanical

forces such as abrasion and grinding break down larger, bulk size particles into smaller nanoparticles (Li et al., 2021c; Stefaniuk & Oleszczuk, 2016). There are also some other physical process types that are still mostly done only on a laboratory scale, such as noble gas sputtering, laser ablation, and severe plastic deformation (Pasinszki & Krebsz, 2020; Valiev, 1999). Noble gas sputtering is the process in which sputtered iron vapor in a noble gas chamber is cooled down, forming clusters of oxidized nanoparticles. Laser ablation is a process of pulsing a laser onto an iron metal surface which vaporizes the already melting iron and, again, by cooling it down, forms nanoparticles later oxidized by either water or air medium, and severe plastic deformation, which is a process of high pressure straining and channel angular pressing to achieve a uniform and fine nanoparticle (Pasinszki & Krebsz, 2020).

On the other hand, chemical process types are bottom-up techniques, meaning nanoparticles are "pieced" together by several chemical reactions (Li et al., 2009). Such process types typically include chemical reduction and aqueous phase reduction (Li et al., 2021c). There are also other less common processes, such as the ultrasound method, where with the power of waves and reduction solution, nanoparticles are formed (Jamei et al., 2013); carbothermal reduction process, which uses a form of iron-containing salts, which are then reduced by high heat in the presence of reducing agents such as carbon dioxide or carbon monoxide in the form of gas (Hoch et al., 2008); vapor deposition, which is a process of heating compounds of organoiron that are easily broken down in a gas phase leading to a production of nanoparticles (Pasinszki & Krebs, 2020); and electrochemical method, which is a fast and simple process using iron-containing salts, electric current, and electrodes to produce nanoparticles that are then removed from the cathode by a cationic surfactant and ultrasonic waves (Chen et al., 2005).

The final category of process methods are the green methods process types, which are made in association with either microorganism, plant extracts, and biomass. The future of this process type is yet to be investigated and implemented on a larger scale, but it is the most promising and is gaining popularity since there are no toxic reducing agents involved (Monga et al., 2020). The basic principle of green synthesis is to implement different environmentally friendly and biodegradable solvents, chemicals, and biowaste while remaining cost-effective, efficient and fast (Kheskwani & Ahammed, 2023).

By using plant extracts and derivatives, especially polyphenols, which are phytochemicals responsible for plant defence mechanisms, this process effectively assists in the nZVI synthesis since they have functional groups responsible for chelating metal ions and suppressing reactions involving superoxides (Monga et al., 2020). Except polyphenols, phytochemicals used in green method synthesis include different enzymes, proteins, cyclic peptides, amino acids, ascorbates, glutathione, metallothionein, ketones, flavonoids, aldehydes, etc., whose concentration and presence depends on the type of plants, thus making the synthesis context-specific (Sharma et al., 2019). General plant-assisted synthesis consists of a plant constituent solution, usually high in polyphenols, due to their ability to control the reduction capacity. The solution is then thermally treated, filtered, and mixed with the iron-containing solution such as ferric chloride, ferrous sulphate, ferrous chlorate, etc. The nanoparticles are formed after the activation phase, which includes a spontaneous combination of negative phytochemical groups with the positive iron metal ions, growth phase, there nanoparticles are chelated, reduced, and nucleated to form zero-valent forms and the right morphology, and in termination phase which contributes to their stabilization in the presence of heat, and lowered agglomerabillity (Kheskwani & Ahammed, 2023).

Further into the aspect of green methods process type, another way of synthesizing nZVI includes the use of microorganisms. A lot of multicellular and single-celled microorganisms like yeast, bacteria, fungi, and algae generate inorganic substances either within their cells or outside of them that can turn metal ions into various metallic nanoparticles (Thakkar et al., 2010; Sastry et al., 2003). Reductive capabilities of different metabolites and proteins residing in them that are responsible for such transformations and nanoparticle production can be altered or improved by altering the temperature, pH, substrate exposure or concentration. But to achieve the best results, the most important factors to follow are picking the right microorganism, preferably ones that naturally accumulate metals and have high enzymatic activities, the best growth parameters, and the best reaction parameters to achieve sustainability and enable larger-scale production. The advantages of such production are beneficial properties of microorganisms, such as generation of secondary metabolites, vigorous multiplication, rapid growth, and enzymatic activities. These properties can contribute to a high potential for large-scale fabrication, but a notable disadvantage of

microorganism nanoparticle production is the complexity of production due to high sterility needs (Monga et al., 2020).

3.2.2 Types of nZVI particles and modifications

As nZVI´s popularity among the science community grew bigger, the research gaps became more obvious, especially in the sense of improving its properties. The creativity in modifying and synthesizing the nZVI became important since its effectivity, both in the laboratory and in the field, is media, species and context specific (Ken & Sinha, 2020). The most important improvement features that should always be followed are improvements in the sense of the range of contaminants it can deal with, improvements in the range of dispersion in the media, improvements in the duration of its lifespan, improvements in the overall efficiency, and improvements in the field of potentiality of combining nZVI with other remediation techniques (MacKenzie & Georgi, 2019).

There are a few types of nZVI particles. So called bare nZVI are particles with no added outer shell except their own iron oxide coating. Their synthesis can be divided into a top-down or bottom-up approach. The top-down approach starts with bigger particles of iron fillings ranging in sizes of micrometres or millimetres, which are then milled into nano-sized particles. On the other hand, the bottom-up approach starts at the laboratory, where different techniques are used, being either physical or chemical; for instance, dissolutions of iron oxides, iron salts, or different iron molecules, from which the most popular and most commonly used is the reduction by borohydride of either Fe(II) or Fe(III). It is a simple synthesis, and for that reason, it is commonly used for commercial purposes (Li et al., 2021b).

Another type of nZVI particles is called bimetallic. It was developed with the purpose of improving its reactivity, so noble metals with catalytic potential were added to it. In the presence of those noble metals, the nZVI particles go through galvanic corrosion, and the production of hydrogen molecules increases. This process helps the particle instigate the reduction of a possibly wider range of contaminants than it would do on its own, for example, potentially risky metals, chlorobenzenes, organic pollutants, etc. The downside of this type of nZVI particle is its lifespan due to the

galvanic corrosion it goes through once the noble metals are added (Kadu & Chikate, 2013; MacKenzie & Georgi, 2019).

The nZVI particles can also be modified by a polymer layer. This modification is made to improve the features of dispersion in the media. The forces made by the organic polymers added on the surface of nZVI particles make the particles repulse each other and prevent agglomeration, which drives the dispersion to further and deeper into the media (Phenrat et al., 2009a). MacKenzie & Georgi (2019) argue that the drawbacks of this type of nZVI particle are the use of synthetic polymers, which can be viewed as contaminants in the subsurface, or polymers, which would coat the particle in such a way that it would lower its reactivity. The different solvents, chloromethanes, chlorobenzenes or tar are considered to be dense non-aqueous phase liquids, which are hard-to-reach contaminants in the media such as soil or groundwater. As such, its sources need a special type of nZVI called emulsified nZVI. Emulsified nZVI is an emulsion of oil, different surfactants, and the particles themselves (Zhang et al., 2019a). They reach such zones in the media through the power of their hydrophobicity and effective reactive aqueous core. The downside of this complex type of nZVI is its delivery techniques. Oftentimes, the dispersion in the soil media is difficult, due to the previously mentioned feature of agglomerabillity of nZVI, so the nZVI particle has to be supported by polymers or different carbon compounds. The supported nZVI is modified based on the context of the media, research and its remediation goals. Usually, the modification is focused on the size and/or improvement of the particle´s surface by changing its charge or adding hydrophobic features (MacKenzie & Georgi, 2019).

3.2.3 Sulphidated nZVI modification and synthesis

The history of sulphidated nZVI starts with the exploration of reductive properties of iron sulphides, which are a broad group of minerals from which it is possible to single out greigite, mackinawite, pyrite, marcasite and smythite. Greigite and mackinawite are the most important and explored in terms of immobilization and control of potentially risky metals in the environment. When comparing iron sulphides with nZVI, iron sulphides provide a lower number of available electrons in comparable dosages. While iron sulphides are more selective towards pollutants, they are less

efficient in the removal of chlorinated compounds than nZVI. Their low reactivity compared to nZVI is due to many other nontarget reactions they go through, but that offers them a higher reduction potential. Looking at the benefits and drawbacks of both, the conclusion is that they complement each other well once modified together (Su et al., 2019).

Findings on the topic of reactivity of sulphidated nZVI started in 2001 due to an increase in the interest in its selective nature towards contaminants. The paper by Su et al. (2019) investigated selectivity towards chlorinated carbon compounds and compounds such as Cd, azo dye, pertechnetate, diclofenac, etc., and they concluded that if the sulphidation of nZVI is increased, the particles become less characteristic of nZVI and more similar to iron sulphides. This leads to a lower reactivity, and depending on the type of contaminant, the optimal ratio needs to be achieved in order to remove them from the environment. This also relates to nZVI´s mobility in porous media, which is low due to settling, deposition, aggregation and magnetism. This is where sulphidation of nZVI is considered because it can lower the electrostatic repulsion and, therefore, magnetization and aggregation.

Synthesis of S-nZVI usually involves two types of methods, one-step or two-step synthesis. However, a third, less commonly used method, the addition of a sulphide in the process of ball milling or precision milling of the iron, may be used (Garcia et al., 2021). For the one-step synthesis method, the solution of sodium borohydride and salts containing sulphur, for example, sodium dithionite or sodium thiosulphate, are continuously dripped into a solution of iron salts where the final product, S-nZVI, is obtained from the solid precipitate. The extent of sulphidation depends on the amount of sulphur contained in salts added to the iron solution, commonly known as S/Fe molar ratio. Which, if it exceeds the ratio of ~0.2-0.3 can lead to demagnetization of the S-nZVI particles. On the other hand, in the two-step synthesis method, nZVI is prepared first, commonly with reduction by a borohydride, and then further sulphidated with agents, such as sodium sulphide or sodium disulphide, or a solution of sodium sulphide and iron salts (Su et al., 2019; Yang et al., 2022).

3.2.4 NANOIRON

The following information was acquired by contacting NANOIRON company, from which the nZVI used in the experimental part of this thesis was used, called NANOFER-25DS. Due to its proprietary nature, the information received was that the nZVI particles in the NANOFER-25DS product are formed by a solid-state synthesis. Except from the information obtained via a direct inquiry, their website states that the NANOFER-25DS is a water-based suspension of zero-valent iron particles and sulphur-containing inorganic compounds, especially efficient in the removal of trichloroethylene. The efficiency of conductivity and hydrophobicity, dispersibility, non-corrosive tendencies, and the particles lifespan come from the sulphur modification of the nZVI shell structure (Nano Iron, ©2010).

The subsequent publication by Li et al. (2009) exemplifies the principle of the mentioned solid-state nZVI synthesis. They state that unlike the common solvent synthesis of nZVI with borohydride, which requires the borate byproduct removal and separation resulting in wastewater production, precision milling is relatively simple and requires no additional chemicals resulting in a more sustainable technique. The only drawback of this type of synthesis is the more complex equipment that is needed to mill the product down to a nano size, and the end nanoparticles may be deformed due to the strong mechanical forces. Precision milling works on a principle of heavier metal beads breaking down the micro or milli-meter iron particles for hours while generating a system of cooling and circulation of the suspension. The study´s findings, observed by the scanning electron microscope, show that the particle size, in fact, reached the nano-size under 50 nm after 8 hours of milling, but with irregular shapes compared to chemical synthesis. Besides the size, the surface area determined using the Brunauer-Emmett-Teller analysis (BET) increased by 95% from the starting iron suspension particles. The experimental results also conclude that after exposing the produced nanoparticles to various chlorinated contaminants, they performed better than the nZVI synthesized by borohydride, based on gas chromatography during their degradation. So, the study establishes that after comparing their findings with the common borohydride synthesis, the precision milling synthesis is more environmentally friendly as it produces far less waste and is better in contaminant removal, therefore potentially better for commercial production and *in situ* application.

3.3 Applications of nZVI in Soil Remediation:

nZVI poses great potential as a soil remediation technique in the removal of potentially risky metals due to its low cost and versatile production methods, rather low toxicity, and great reducing capacities (Jiang et al., 2018). An important nZVI property is its very diverse and easily modifiable nature, which allows scientists to target specific contaminants and work in different environments and types of soils. Mechanisms of transformation, complexation, and adsorption, which are the main modes of action to remove soil pollution, organic and inorganic, and a potential to avoid secondary pollution by removing nZVI with the forces of magnetism or gravity due to its iron content (Li & Luo, 2020). The following sections will explore and review research efforts focused on successful nZVI applications in soil remediation, with an emphasis on recognizing different specific conditions and target objectives to provide context insight.

3.3.1 Soil contamination by potentially risky metals

Soil contamination by potentially risky metals is caused by their lasting presence in the environment, tendency to bioaccumulate, and overall toxic nature. Their natural origin is weathering and erosion of metal-containing rocks and bedrock and volcanic activity. Anthropogenic origin comes from activities related to farming, the use of different fertilizers and pesticides, industry, mostly from fossil fuel combustions and mining, such as smelting and ore processing activities. Anthropogenic activities contribute to the disruption of their natural biological and geological cycles, allowing potentially risky metals to enter the food chain and portray great health and environmental concerns. Even though they are essential to life, their absence or excess pose risks. Potentially risky metals easily contaminate different ecosystems, whether aquatic or terrestrial, due to their persisting and accumulative nature, further making their trophic transfers of great concern (Ali et al., 2019).

3.3.2 Geochemical properties of soil and their interactions with nZVI

Experimental evidence showed that there are many different factors that can influence nZVI´s performance. Common factors include the type of pollutants and the type of nZVI. But in the context of soil remediation and potentially risky metal

removal, more complicated geochemical factors play role, e.g., contact time and reaction time, pH, standard redox potential, soil organic matter content, already present soil ions, and cation exchange capacity (Hong et al., 2022; Alazaiza et al., 2022).

One of the key factors influencing the performance of nZVI in soil is the pH. Depending on the value of the pH, it can affect the removal mechanisms, its iron core´s surface charge, or levels of ionization or speciation of potentially risky metals. At low pH levels, nZVI surface becomes more positive, therefore, it electrostatically repulses positive metal cations but improves the adsorption of anions. In contrast, high pH levels lead to the creation of hydroxides, which more easily react with cation species complexes (Alazaiza et al., 2022).

The cation exchange capacity of soil is related to the pH factor. Its changes depend on the soil type, and its levels can lead to improved or worsened reduction of contaminants by nZVI due to chemical complexations and ionic exchanges that lead to lower potentially risky metal concentrations available for efficient removal (Hong et al., 2022). In the study by Yaacob et al. (2012), they observed that cation exchange capacity does not correlate with the specific surface area of the nZVI used. Rather, Huang et al. (2021) observed that it correlates with pH but negatively correlates with the organic matter content of the soil. The organic matter content dropped with the oxidation of nZVI, but pH and cation exchange capacity increased due to less functional groups found in the organic matter, which naturally ionize the hydrogen ions leading to a decrease in pH. The target contaminant Cd changed to a stable form, and a higher number of iron oxides positively correlated with the increase of pH and cation exchange capacity.

Soil organic matter involves humic and fulvic acids whose charges can influence and compete with the nZVI to remove potentially risky metals. The derivatives of the humic acid, such as phenate and carboxylate groups, compete with nZVI in a way that they form complexes with potentially risky metals prior to nZVI. Therefore, organic matter high-content soils are not preferable for nZVI remediation (Alazaiza et al., 2022).

Interestingly, Wang et al. (2021a) noted a decrease in both dissolved organic carbon and dissolved aromatic carbon in their study after treating the soil with nZVI. The decreased dissolved organic carbon is, presumably, due to the inhibition of

decomposition by microorganisms by nZVI, and the decreased dissolved aromatic carbon is, presumably, due to nZVI adsorption because of competitiveness between the contaminants and dissolved aromatic carbon.

A study by Wang et al. (2020) investigated the relationship between soil organic matter, nZVI, and clay particles, and their potential to form complexes and interfacial interactions. The interaction between soil organic matter and nZVI is based on moieties, usually aromatic, of soil organic matter that easily adsorb on the nZVI´s surface, based on high molecular weight (Li et al., 2018). On the other hand, clay minerals and nZVI interact on Lewis´s acid-base or electrostatic interaction basis depending on the pH of the environment. In the soil solution, soil clay mineral montmorillonite and kaolinite aggregated with nZVI, therefore altered the clay mineral and dissolved organic matter interfacial interactions. The nZVI and clay mineral aggregates sequestrated organic carbon leading to potential alterations in nutrient and contaminant cycling in the geochemical systems (Wang et al., 2020).

The next key factor Alazaiza et al. (2022) mention is contact time, especially in the case of adsorption mechanisms. The efficacy of removal is high, and it depends on the potentially risky metal species until all of the active sites on the iron oxide shell are used up, then it starts to slow down or comes to a stop, or until nZVI is aged and its surface starts crystallizing. In the study by Chen et al. (2020), where they investigated the efficiency of Cr(VI) removal with bimetallic modified nZVI and copper, the results showed that lower pH is much more favourable. The low pH is favourable due to Fe^{2+} release causing an inhibitory effect on the iron oxide deposition on the surface; therefore, more active/contact sites for the reduction of Cr(VI) are available. On the other hand, the higher pH levels in the soil lead to formation of a passivation layer on the bimetallic nZVI therefore more and longer contact with Cr(VI) is limited.

Not only does the soil´s standard redox potential indirectly affect the solubility, mobility, toxicity, oxidation states, and bioavailability of potentially risky metals, but it also affects nZVI removal efficacy and performance (Mao & Ye, 2018; Alazaiza et al., 2022). As nZVI´s standard redox potential is very high, it can interact not only with potentially risky metals but also with different components, such as dissolved oxygen or other electron-accepting components in the environment (Alazaiza et al., 2022). On the other hand, Wang et al. (2021a) found that the standard redox potential

of the soil decreased because of the consumption of oxygen by nZVI and its reductive nature and then later increased due to the further oxidation of nZVI and its products, the secondary minerals of iron.

Soil´s standard redox potential leads to the next key factor in nZVI´s performance, already naturally existing and co-existing anions and cations in the soil. Co-existing anions and cations in the soil compete for the active sites with target contaminants that have to be removed, or rather, they act as catalysts or inhibitors for removal processes directed by nZVI (Alazaiza et al., 2022). For example, in the study by Zhu et al. (2017), they found that some co-existing ions affect the removal of Cr(VI) in the soil leachate while others do not. The nZVI and nickel bimetallic particles were negatively affected by SO_4^{2-}, HCO^{3-} and CO_3^{2-}, while there was no effect in the presence of NO^{3-} ions. The reason for the inhibitory effects of those ions varies, CO_3^{2-} formed complexes on the surface of the nZVI, therefore competed with the contaminant, while HCO^{3-} in acidic conditions reacted with hydrogen ions, increasing pH, which, as previously mentioned, is not favourable for reduction environment.

The behaviour of nZVI in soil pore water is a series of transformations. Usually, nZVI in soil pore water goes through oxidation, forming iron hydroxides and iron oxides, which deposit on the soil particles. The nZVI that does not oxidize, usually due to a modified surface, either migrates further in the system, reaching target contaminants, or forms homoaggregates and deposits on the soil particles (Wang & Lin, 2017). In the case of heteroaggregates in the study by Wang et al. (2021a), they found that the clay mineral-nZVI aggregated structures were also dependent on the soil moisture content. The higher it was, the more such structures formed due to sped-up oxidation of the iron core because higher moisture content reduces and hydrates the iron oxide shell. Also, the smaller nZVI they used aggregated more with the clay minerals and oxidized less even under high soil moisture contents. Regarding the iron speciation distribution, iron species decreased mainly as the soil moisture content was increased, which caused the oxidation of nZVI to be increased, but the oxidation products, hydroxylated iron oxides, pose no further risk to the environment. Soil pore water´s inorganic and organic colloids and nZVI make heteroaggregates due to their pH dependency, different charges, and large specific surface area. Exposure to water for a longer period of time in an environment can also alter the nZVI´s ability to reduce

pollutants due to the hindered transfer of electrons from the core to the surface (Wang & Lin, 2017).

The nZVI and soil interactions are concurrent. Therefore, the nZVI´s transformations, influenced by different geochemical factors, are also dependent on the different soil properties and types for its performance. The results from the Wang et al. (2021a) study showed the changes that nZVI goes through regarding morphology in acidic soil from the city of Hangzhou are developments of chain-like aggregates of nZVI that prefer lower clay mineral electronegativity. But, the same aggregates, after some aging time in the soil, dissolved, collapsed, cemented, and made complexes with soil particles. With further aging time, these complexes led to micrometre structures of soil particles and cemented nZVI aggregates.

Another article by Liu et al. (2019) investigated how, during soil decontamination of lead, nZVI interacts with quartz as a common inert soil mineral. Even though the corroded nZVI precipitated on the quartz minerals in the forms of plush and flake clusters, the shape or the shear strength of the quartz was not compromised. Therefore, they concluded that nZVI remediation in soil does not interfere with the geotechnical strength of soil.

3.3.3 Cd, As and Cr(VI) immobilization by S-nZVI

Recent studies have focused on the ability of nZVI and S-nZVI to immobilize potentially risky metals. Three studies in the past 3 years have focused on the immobilization of Cd, As, and Cr, respectively. In all three of these studies, the S-nZVI was prepared by chemical synthesis with a sodium borohydride. The findings of these studies allow for a greater understanding of the applications of nZVI and S-nZVI in soil remediation regarding potentially risky metals (Guo et al., 2021; Han et al., 2021; Liu et al., 2023).

The article by Guo et al. (2021) investigated how effective S-nZVI can be in immobilizing Cd in efforts to remediate the highly polluted agricultural lands in China. The focus of the study was on Cd pollution, which is present in the soil as either carbonate-bound, organic matter-bound, iron manganese oxides-bound, exchangeable or as in residual fractions (Guo et al., 2021; Tessier et al, 1979). Since bare nZVI is not efficient enough to immobilize Cd due to Cd not being able to pass through the

oxide shell, sulphidation of nZVI is introduced to surpass this inefficiency because it improves the selectivity, electron exchange, and conductivity for better remediation efforts with potentially risky metals (Guo et al., 2021). For the same reasons, the study conducted by Han et al. (2021) researched pentavalent As immobilization success of sulphidated and bare nZVI in soil, and Liu et al. (2023), remediation of Cr(VI) soil pollution by S-nZVI, in hopes to circumvent the bare nZVI´s side reactions with water, which usually result in challenging hydrogen gas production, and its impact on the microbial communities present. The soil in all three experiments was spiked artificially and nZVI was added in slurry form. The soil was spiked with a solution of Cd Cl in the ratio of 1:1 to achieve the 49.5 mg kg^{-1} concentration of Cd, followed by the addition of 0, 1, 5, and 10 g kg^{-1} S-nZVI slurries, respectively, in sets of batches with predefined time periods (Guo et al., 2021). Artificial soil made from sand, peat moss, clay and calcium carbonate in a ratio of 69%, 10%, 20% and 1%, respectively, was spiked with As and mixed with the nanoparticles in 0%, 0.3%, 1% and 5% (w/w) (Han et al., 2021), and farm soil from the city of Zhejiang was introduced with a Cr spike in a 1:1 solution ratio (Liu et al., 2023).

The conclusions drawn from Guo et al. (2021) are the following. The exchangeable Cd availability was the lowest at the 5 g kg^{-1} of S-nZVI in a 30-day interval, turning it into iron-manganese-bound and organic matter-bound Cd species, which are less available and less toxic compared to the exchangeable Cd. The conclusion from the pH measurements showed that the initial soil pH had negligible effects on the immobilization of Cd in any of his chemical fraction forms. The immobilization mechanisms results showed pathways of iron, oxygen and sulphur elements playing well in the immobilization of Cd via adsorption, precipitation and reduction. Through all the combined results of the study, S-nZVI can indeed be used for efficient Cd removal and, therefore, used in soil remediation of their target agricultural soils in China.

Once the soil was introduced with S-nZVI in the study by Liu et al. (2023), the nanoparticles showed great mobility compared to the bare nZVI, which could not pass through the silica sand in the soil due to bigger aggregation and magnetization. The efficiency of S-nZVI proved to be higher than the efficacy of bare nZVI by 14%. This can be attributed to iron sulphides present on the iron oxide shell of S-nZVI that increase the electron transfer and, therefore, the affinity of S-nZVI to react better with

Cr(VI). Also, Cr fractionation was investigated after the treatment with S-nZVI, which showed that the Cr species converted to organic matter bound. As previously mentioned, the sulphidation improves the electron transfer and, therefore, the reactivity and selectivity for Cr. This is followed by a reduction mechanism on the surface by iron sulphides leading to the production of Fe(II) and iron oxides, which also have a role in immobilization. Regarding the microorganisms, they showed a mutual impact with the S-nZVI and were less affected in terms of cytotoxicity than in the presence of bare nZVI.

Interestingly, due to a lack of research data on this topic, an artificial neural network was introduced in the study by Han et al. (2021), which they trained to predict and evaluate the effectivity of both nZVI and S-nZVI, by inputting the treatment and dosages and getting output on the immobilization success through the application called MATLAB_R2018b Neural Net Fitting. They also performed X-ray analyses to show remediation mechanisms and the toxicity of this type of nano remediation based on the earthworm survival in the spiked soil. It became evident that the decrease of As content by S-nZVI in the soil pore water was lower than of nZVI, presumably based on the larger specific surface area of nZVI, based on the Langmuir isotherm model. But, S-nZVI performed better by almost double the success in adsorption once the surface area was normalized in the soil and water, based on the Freundlich isotherm model. Therefore, sulphidation does indeed improve the immobilization of As but is dependent on the available surface area. Although soil by itself made complexes with As, the decreased leachability of As was noted once nanoparticles were introduced, meaning that there is a stronger affinity for As to bind to them rather than to soil particles. In the S-nZVI treated soil, there was also evidence that sulphidation improves As removal because both sulphur and iron compounds helped to co-precipitate As and make As_4S_4 and FeAsS. This important aspect of As removal mechanism by co-precipitation of As is crucial for its immobilization, supported by the sulfhydryl groups as binding sites, and S/Fe molar ratios. They also observed that even though the kinetics of S-nZVI in immobilizing the As is slower than nZVI, it is still more effective than nZVI, and that their kinetics become similar over time. Examining the outcomes of the artificial neural network, they discerned that it is possible to model the immobilization of As and that this can be further used for other remediation predictions, especially for deliberation in field studies, but taking into

account more specific soil parameters as input information for even better results. Regarding the earthworm survival during remediation with nZVI and S-nZVI, they noted their survival dropped regardless of the treatment time or the type of nanoparticle. They conclude that even though both nZVI and S-nZVI can be successfully used in nano remediation of soil, the sulphidation does improve the immobilization of As and lessens the toxicity, therefore making S-nZVI a more promising particle.

3.3.4 Mobility and transport of nZVI in soil

Mobility and transport of nZVI can be explained through theories related to the movement of particles in the soil and their interactions with other soil constituents. Although research on the mobility and transport of nZVI in soil is limited, it mostly regards groundwater, which will be explained in the following sub-chapter through the physics of nZVI mobility and transport in porous media.

In general, the mobility of nanoparticles, therefore nZVI, takes place in the soil pores rather than by settling due to gravitational forces, although not excluded. Once the nanoparticles enter the soil, they occupy a pore space where they bind to either a colloid or a contaminant, which will further transport the particle. Mobility is highly dependent on the soil properties, such as ionic strength, humic acids content, and the presence of water, and particles´ properties, such as size and shape. In contrast, if it does not meet the right conditions or if it does not bind with a mobile constituent, its transport will probably not occur, and it will aggregate (Belal & El-Ramady, 2016) or deposit (Yusuf et al., 2024).

A study by Li et al. (2023) highlights that *in situ* application of nZVI faces challenges and limitations in its agglomeration and colloidal system role and in its iron oxide shell passivation. Agglomeration of nZVI arises from its magnetic properties due to its iron nature, but it can also be contributed by its mutual collisions in the soil media, especially if found in large concentrations, or if its electrostatically repulsive effect is reduced by magnesium and calcium ions in the soil pore water.

Another reason for the agglomeration of nZVI can be explained by the Derjaguin, Landau, Verwey and Overbeek theory or short DLVO theory, more so the extended DLVO theory. The DLVO theory explains that the electrostatic interaction between particles in a colloidal system is a result of the particles´ closeness and

overlapping of their layers. So therefore, it is a measure of colloidal stability because of the particles´ van der Waals attractive forces and repulsive electrical forces. The Extended DLVO theory, unlike the DLVO theory, also includes the effects of the acid-base interactions, hydrophobic interactions, and effects of hydration (Ohshima, 2012). Jiang et al. (2015) studied how the aggregation of nZVI would be influenced under limited and sufficient dissolved oxygen available in a colloidal system also using extended DLVO theory. nZVI oxidized in a sufficient dissolved oxygen environment shows good colloidal stability while nZVI oxidized in limited dissolved oxygen environment shows bad colloidal stability and tends to aggregate more. The reason for bad colloidal stability was explained through increased magnetization levels of different oxidation states in a limited dissolved oxygen environment, supported by the extended DLVO theory directing the aggregation configuration.

The mobility of nZVI can also be explained through flow rate, interaction with collectors, pH, filtration theory, Brownian movement, and grain size of the porous media (Yusuf et al., 2024). The soil texture and flow rate´s influence on mobility was studied in the article by Ye et al. (2021). By increasing the flow rate, the mobility of colloids increases due to better hydrodynamic forces. Regarding the soil texture, sandier soil leads to better mobility compared to soils containing more clay due to the higher adsorption capacity of soil. Organic matter in the soil also contributes to nZVI´s mobility as it is a good collector, which reduces the stickiness, enabling further *in situ* injection of the nanoparticles (Johnson et al., 2009). Filtration theory or Darcy´s law, in the porous media, describes the flow rate of liquids in the micro and macro pores of soil. The holding capacity of nanomaterials, due to their complex nature, can also be explained through mechanisms of interception, which is direct contact with the soil particles, gravity-driven sedimentation, and Brownian movement, which explains the randomness and potential diffusion of nanoparticles (Yusuf et al., 2024).

3.3.5 nZVI related challenges and limitations

The article by Chekli et al. (2016) investigated the contaminant co-transport by nZVI using radiolabelling. The goal of this study was to see if modified nZVI, due to its stability, can facilitate such co-transport in chromated-copper-arsenate contaminated soil. The findings showed that polymer-modified nZVI stayed in the

topsoil in the retention profile, meaning in case of soil remediation by nZVI, it is better to inject it into the topsoil to avoid the risk of co-transporting contaminants into the subsoil. Again, due to the context specificity of nZVI, the other scenario would be if nZVI is not injected into the topsoil but rather injected deeper or mixed in with the soil. Due to the colloidal co-transport and adsorption of the soil system, it would also co-transport contaminants to some extent. Nanoparticles´ mobility and transport drives are usually based on models rather than experimental examples. Regardless, they can serve as a background for the *in-situ* studies. Due to the natural iron presence in soil systems, it is hard to track the mobility of nZVI and to state its actual positioning. To overcome this issue, radiolabelled nZVI is implemented to track it in the soil profile cores and contaminated soil. The radiolabelled nZVI can also be modified with carboxymethyl cellulose to improve its stability in the soil media. The transport is rather low in terms of mobility, as the particles tend to stay in the topsoil, which is in regards to the type of soil used (Chekli et al., 2016).

Transport and mobility issues also lay potentially in the accumulation and retention of nZVI in soil. Zhang et al. (2019b) note that retention is caused by adsorption of nZVI by the soil system. Even though the adsorption by soil particles is often represented as a transport issue, the colloidal co-transport, like in the case of co-transport of contaminants in the soil, may also occur in the case of nZVI transport. The nZVI adsorbed in all three types of soil that they used, typic-hapli-udic argosols vertic shajiang-aquic cambosols, and typic ochri-aquic cambosols, but to show the co-transport via soil colloids, sandy soil, diatomite and quartz sand were used. The readings from the breakthrough curves showed that the soil colloids indeed facilitated the co-transport. Therefore, nZVI treated water or similar, if disposed in soil, can lead to expanded pollution area. But, the co-transport of nZVI also means, deeper and better reachability of contamination zones in soil systems. Except the soil colloids, there is also a possibility of artificial dispersants, such as polyacrylic acid, which improves the distance the nZVI can be transported in the soil matrix of silica sand (Yang et al., 2007).

One of the challenges of nZVI remediation is its potential toxicity. Even though there are many scientific articles regarding its toxicity, due to its high context-specific response, it still remains fairly unknown. In an article by Fajardo et al. (2015), they investigated the after-remediation consequences of aged nZVI in soil polluted with

lead and Zn. While the Zn-remediated soil showed stimulating biodiversity influence, the lead-polluted soil showed oxidative stress that led to low cellular activity of microbes and stunted growth in *Caenorhabditis elegans.* While the remediation was successful, and the geochemical properties of soil improved in levels of nutrients and iron, the findings of this study show that the context-specific nature of nZVI and its toxicity lay even on the level of the contaminant.

The nZVI passivation is positive in the sense of contaminant removal mechanisms and in the formation of beneficial byproducts, which can also further reduce contaminants, such as mineral phases of iron such as goethite, hematite, vivianite, surface-bound Fe(II), etc. But passivation can also lead to the formation of toxic byproducts, but through further modification of the nZVI´s shell, negative passivation byproducts can be mitigated or even lead to further production of positive passivation byproducts. The passivation chemistry and byproduct formation lie in the context of the environment. Some negative byproducts that can arise from nZVI passivation are reactive oxygen species, which are oxidative stressors for higher plants, leading to plant responses in the form of enzymatic and non-enzymatic resistance mechanisms (Bae et al., 2018; Saed-Moucheshi et al., 2011).

3.4 Reactivity Mechanisms and Environmental Fate of nZVI in Soil:

3.4.1 Basic principles of removal mechanisms by nZVI

Even with the wide array of nZVI research conducted, there is still no clear or definite way to explain the complex interactions between potentially risky metals and nZVI. There still exists a gap in the agreement of the information that could define such interactions due to the complexity and context dependency of each experimental treatment of remediation (Alazaiza et al., 2022). Latif et al. (2020) summarized the elements belonging in the four main types of interactions: adsorption mechanism (Cr, Pb, U, Ar, Se, Ni, Co, Zn, Cd, Ba), reduction mechanism (Cu, Cr, Ar, Ni, U, Se, Pb, Hg, Pu, Ag), oxidation mechanism (U, Ar, Pb, Se), and precipitation interaction mechanism (Co, Cu, Zn, Cd, Pb). Potentially risky metals can be affected by multiple mechanisms due to the sequential process of removing them via nZVI-supported remediation.

The adsorption mechanism is a low-cost and safe mechanism of removal based on the standard redox potential. The more similar or more negative the redox potential of an element, the more likely it is to be adsorbed. Iron oxides on the nZVI´s shell, many functional groups, and active sites are responsible for the adsorption of metals and metalloids (Alazaiza et al., 2020). The mechanism of chemical reduction is more commonly occurring in aqueous media where potentially risky metals, once in the presence of the zero-valent core, are reduced to lower oxidation states (Tarekegn et al., 2021). The zero-valent iron core donates electrons, lowering the potentially risky metals´ oxidation number and lowering its mobility and toxicity; it is considered a direct way of reducing a contaminant. The steady reduction occurs after the adsorption mechanism, where the Fe(II) is responsible for further reduction. Less common and environment-specific is the oxidation mechanism, which only occurs if the Fenton reaction is viable and if there is a presence of oxygen. The principle of this mechanism is based on the derivatives produced by the zero-valent core, which can be of an oxidizing nature. The last interaction mechanism that is going to be mentioned is the precipitation mechanism. It is the most variable mechanism occurring sequentially or simultaneously with adsorption and reduction (Alazaiza et al., 2020). Firstly, the metal ions of nontoxic nature replace the chelated metal ions, which are then precipitated by nZVI (Latif et al., 2020).

3.4.2 Pollutants removal mechanism pathways of nZVI

In the insightful analysis by Ling et al. (2017), they mapped out nZVI´s reaction mechanisms with Cs(I), As(V), Ni(II), Zn(II), Ag(I) and Cr(VI) ions using X-ray energy-dispersive spectroscopy scanning transmission electron microscopy (XEDS-STEM) as it provides a new and direct way to identify nanophase mechanisms of interactions which are mediated by the surface reactions rather than solution reactions.

Through XEDS mapping and HAADF imaging of the aftermath of the Cr reduction by nZVI. Their findings showed that the particles still maintained their iron cores and oxide shell structures, although somewhat spherical, but with a distorted, thicker, and deposit rich shell. The reaction mechanism is reduction of Cr to $Cr(OH)_3$, oxidation of nZVI to iron oxides, and iron oxides reactions with Cr (III) hydroxides,

mapped out in the core of the nZVI. Yet, after the reduction of As by nZVI, the nZVI particle composition still remains distinguishable, except for one change. A newly formed 1-1.2 nm layer that lays on top of the iron core is comprised of the reduced As and iron-oxide-As surface complexes.

Hence, their conclusion is that the anions containing oxygen, both Cr and As, first transform on the surface of the nZVI particle due to breakage of the metallic and oxygen bonds followed by diffusion into the oxide shell, where they are reduced. The higher standard redox potential of Cr, therefore a bigger difference than the one of nZVI, leads to a deeper diffusion into the oxide shell and the core, unlike As with the lower redox potential where the transformations occur on the iron core.

The consequences of nickel reduction by nZVI, through XEDS mapping and HAADF imaging, lead to a doughnut resembling shape of the particle. Via iron mapping, the iron deficient iron core shows as a dark area with some of the protruded nickel, while the thick iron oxide shell shows two dimmer layers, one from nickel accumulation on the iron core and one of iron oxides. The void appearing zero-valent iron core is presumably caused by several factors. The first factor is the reduction of nickel, which causes a change of particle properties and fast oxidation of the core. The iron core is the main electron donor for the reduction of nickel, therefore making it appear used up. The next factor is the similarity of the nickel standard redox potential to iron, making nickel diffuse into the core for a faster reaction. The last factor is the so-called Kirkendall effect, which, due to the speed of iron ions transport outwards, leaves voids where the slower nickel atoms cannot catch up with its flow inwards. This speed of iron oxidation and kinetics of the ions is due to several different particle properties, such as size or crystallinity. They also examined the outcomes of the reduction of silver by nZVI using XEDS mapping and HAADF imaging. The following was revealed: lack of the typical structure and distortion is due to changes of the reactions of electrochemical reduction, ionization of the iron, hydroxide precipitation and silver deposition. More so, it also reveals that the reduced silver remains on the surface of the particle encasing nZVI due to the speed of reduction reactions because of silver being such a strong oxidizing agent.

In contrast to the mentioned examples of reduction reactions with nZVI, they also noted and examined the reactions with caesium and Zn, which, due to their much lower standard redox potentials, do not go through reduction but rather precipitation

and sorption. Caesium was found by mapping to be apparent throughout the whole nZVI particle, indicating sorption, but due to its large size, it mostly accumulated on the boundary of the iron core. The Zn reaction with the nZVI, on the other hand, shows Zn agglomerates throughout the nanoparticle. Adsorption into the nZVI particle is governed by pH. The higher the pH, the more precipitation of Zn happens in a solution in the form of Zn hydroxides. As previously mentioned, a change of pH facilitated by corrosion of the nZVI particle further contributes to its speed and effectivity (Ling et al., 2017).

3.5 Interactions between nZVI and Plants:

3.5.1 Influence of nZVI on plant growth

The nZVI exhibits significant potential for promoting plant growth via increased plant biomass and length (Cui et al., 2023). Its stimulatory effect, if used in proper dosage and a controlled environment, can be shown through its ability to serve as a plant micronutrient and disease suppressant (Tolaymat et al., 2017). Especially in contaminated soil, where plants are exposed to more stressors, nZVI improves the conditions by decreasing the concentrated buildup of pollutants, introduces sources of iron, and in collaboration with other agents used in soil remediation, it can improve microorganism activity; therefore, leading to plant growth and increased biomass (Cui et al., 2023). Tomato seedlings exposed to Cd spiked soil showed lessened biomass and growth until 2.5 mg Kg^{-1} of nZVI was introduced. The nZVI counteracted Cd stress and increased seedling height, biomass of roots, and hypocotyledonous diameter (Anwar et al., 2024).

There are multiple factors to consider in interactions between nZVI and plants. Soil is a better media for phytoremediation since nZVI forms fewer coatings on the roots of plants than in water, where the dispersion is freer. nZVI´s effect on plants is also dependent on the synthesis type. Green synthesis of nZVI has shown more positive and improved seed germination rates, as well as increased biomass and plant length than the borohydride synthesis method. Another important factor that affects plant growth in the presence of nZVI is the concentration. The overall trend observed in nZVI and plants interaction is that the low dosage usually leads to stimulating effects, while the high dosage usually leads to inhibitory effects. High nZVI

concentration can lead to rapid release of oxygen in the soil. Due to changes in the redox states, it affects the roots and with that, also the plant growth. Change of microorganism biodiversity can be affected with large concentrations, from which many are a part of the ecosystem that promotes plants health and growth (Cui et al., 2023).

Seed germination development and rate are important first steps towards plant growth. The main factor determining germination rate in regards to nZVI is the dosage in which it is applied. While the high dose, over 1000 mg L^{-1}, of both bare nZVI and starch stabilized nZVI showed inhibitory effects on the seed germination of mung bean (*Vigna radiata*), the decreasing concentrations of bare and starch stabilized nZVI showed a decreasing rate of inhibition on the seed germination (Sun et al., 2019). Similar results were obtained also in another study, germination rate at 1000 mg kg^{-1} and 1500 mg kg^{-1} of nZVI showed inhibitory effects for *Kochia scoparia,* while 500 mg kg^{-1} of nZVI as stimulatory (Zand and Tabrizi, 2020).

Similar factors need to be taken into account while discussing root and shoot growth of plants exposed to nZVI. Root and shoot morphology are mostly affected by rising nZVI concentrations. For example, rising levels of nZVI in supported lead decontamination reduced the root biomass of *K. scoparia,* while at lower levels from 100-500 mg kg^{-1} it stimulated root length growth (Zand & Tabrizi, 2020). On the other hand, nZVI type factor can also affect the root and shoot morphology. The effects of the bare nZVI and starch stabilized nZVI differed in the shoot and root morphology of the mung bean (*Vigna radiata*). Starch stabilized nZVI, unlike bare nZVI which showed simulating effects in shoot and root growth at high doses, had different effects at different doses. High doses showed to be simulating for root and shoot elongation, inhibitory at medium doses, and at low doses no effects (Sun et al., 2019).

3.5.2 Transport and uptake of nZVI within plants

There are a few distinct potential pathways for nZVI uptake and translocation within plants. nZVI can enter through root cells in soil and enter the epidermal cells, further translocating through the plant´s cortex. Apoplastic pathways are another way of nZVI transportation in plants, alongside phloem and xylem vascular tissues (Wojcieszek et al., 2023).

The nZVI induced cytotoxicity can be contributed by the size of nZVI, where particles under 50 nm can enter the plant cells where they cannot be removed, therefore leading to cell death, and time of nZVI exposure, especially during seed germination and growth of seedlings (Cui et al., 2023). Except for the small size factor of the metallic nanoparticles in the uptake, there is also an ongoing investigation of instances where the nanoparticles are bigger than the size exclusion limits of the root pores and barriers and they still manage to pass through. Presumptions in case of large nanoparticles that pass though the root barriers are possible plant wounds, modified and flexible barriers, and pectin-filled cell wall networks reduced in the presence of reactive oxygen species, which occurs in stressful environments and leads to a cell wall modification in the size of its pores. In the presence of reactive oxygen species, there is a possibility of polymers splitting in the cell wall, allowing it to loosen up (Ma & Yan, 2018).

If the entry way is through foliar application of nZVI, it is absorbed by leaves through trichomes and stomata. The pathway to the roots is then followed by transport through phloem vascular tissue. Plant species, growth media, and nZVI concentration are further responsible for plant response to nZVI application (Wojcieszek et al., 2023). Another factor in the uptake of metallic nanoparticles are the environmental conditions, such as the concentration of organic matter present. Even though the plant species and the organic matter concentration are complementary, the higher the organic matter concentration usually is, the higher the uptake by plants. Soil salinity, inorganic and organic compound presence, drought stress, and the presence of different microbe communities are some of the other factors affecting the plant nanoparticle uptake, although there is still a lack of information regarding the mechanisms behind them, especially how the root actually internalizes the nanoparticles and how they transport, and therefore it is important to investigate the field results more than the controlled laboratory results because they may drastically differ (Ma & Yan, 2018).

An example of such difference that could arise between *in vitro* and field study was studied by Wojcieszek et al. (2023). *In vitro* experiment showed high accumulation of iron in the roots of *Arabidopsis thaliana* induced by nZVI (Nanofer STAR), leading to increased toxicity, while in the soil media, there were no reported signs of toxic effects of nZVI even though increased accumulation of iron was noted

in plant tissue over time. The nZVI contributes to the iron content that plants can uptake, but with increasing concentrations of nZVI, therefore iron concentrations, it leads to plant malnutrition and decreased absorption of water since it starts blocking the pores of the plant´s roots (Cui et al., 2023). Conversely, sulphidated nZVI (Nanofer 25S) treated plants showed no uptake or transportation of iron or nZVI accumulation (Wojcieszek et al., 2023).

3.5.3 Nutrient and potentially risky metal uptake by plants

The meta-analysis by Cui et al. (2023) stated that nZVI does indeed support the uptake of nutrients and iron by plants during remediation processes. The proof lays in the noted adsorption of nutrients such as K, Mg, Zn, S, etc., which can be found after the nZVI application in the roots and shoots of plants. In the study by Sun et al. (2019), they observed that the mung bean plant roots exposed to starch-stabilized nZVI exhibited higher concentrations of Mg, N and Fe, while those exposed to the bare nZVI exhibited higher concentrations of Mg, P, Fe, and Ca. There are a couple of assumptions about how plants can acquire micronutrients through nZVI nanoparticles. Because iron is less soluble in soil, along with its hydroxides and oxides, there is a possibility of implementation of microbes that can bind the metals to their ligands and make them more easily available for plants to uptake or by making them more soluble by acidifying the rhizosphere (Tolaymat et al., 2017). Nano priming is another example of how nZVI can improve the uptake of micro and macronutrients such as Fe, Zn, Mn, Ca, Mg, Zn, etc. In the study by Guha et al. (2022), they primed the seeds of *Oryza sativa* L. cv. Gobindobhog with nZVI as a way to avoid synthetic fertilizers that often contain potentially risky metals harmful to the environment. The nZVI primed seeds showed to be a much more sustainable nutrient delivery approach for plants, aside from the fact that it also drastically improved the crop yield.

Potentially risky metal uptake and transport are also important aspects of uptake dynamics in plants. Anwar et al. (2024) discussed Cd transport in plants through divalent cation transport, as Cd-specific channels in plants do not exist. As divalent cations, they presume that Cd would also travel through vacuolar iron transporter, iron-regulated transporter, yellow stripe-like transporter, and natural resistance-associated macrophage protein (Sebastian & Prasad, 2018). Due to this type

of transport, it competes with essential nutrients, impairs absorption, and takes over their transport channels. With nZVI introduction, they noted that tomato seedlings were once again high in the nutrient contents in their leaves and roots, compared to Cd spiked grown ones meaning nZVI greatly supports homeostasis of nutrients (Anwar et al., 2024).

The uptake of potentially risky metals by plants and how nZVI assists in it leads us to potential nZVI-assisted phytoremediation. Calculating the translocation factor of a plant is a leading tool that enables researchers to determine if the plant has the potential for phytoremediation. It is given by a ratio of element concentration in the shoots and roots of a plant (Nirola et al., 2015). In the study by Zand and Tabrizi, (2020), translocation factor increased with nZVI application. The 500 mg kg^{-1} of nZVI was the optimal amount to increase the translocation of lead, higher amounts of nZVI lead to inhibitory effects on translocation in *K. scoparia*. Lead only translocated into the roots of *K. scoparia*, while aerial parts remained lead free. They proposed this phenomenon to be due to root apex blocking potentially risky metals. Near the roots apical meristem, apoplastic barriers form and reduce the translocation due to low porosity (El-Temsah et al., 2016).

3.5.4 nZVI induced cellular and intracellular changes in plants

Reported studies on the cytotoxicity in plants noted that nanoparticles may pose risks through DNA strand breaking, anomalies in chromosomes, micronuclei or nuclei, metabolic dysfunction, etc., led by reactive oxygen species occurrence (Gou et al., 2010). Cytotoxicity of nZVI was explored by Ghosh et al. (2017) through changes in cytogenetics, DNA damage, reactive oxygen species production, and potential cell death. Some potential harmful processes were discussed based on the study on *Allium cepa* plant. Firstly, nZVI is dissolved into Fe^{2+} and Fe^{3+} ions, which adhere to *A. cepa* root cells. Once entered the cell via cellular uptake, nZVI and Fe^{2+} and Fe^{3+} induce cytotoxicity through direct DNA damage or indirect DNA damage due to reactive oxygen species production. Abnormalities followed by DNA damage are structural changes due to chromosomal abnormalities. Free radicals produced in the mitochondria are a result of partial oxidation of nZVI, whose Fe^{2+} ions undergo Fenton reaction. Free radicals harm the mitochondrial membrane and its membrane potential.

Plant cell wall loosening induced by the free radicals also leads to root elongation. Furthermore, cell membranes start to leak electrolytes due to lipid peroxidation. Oxidative stress arising from such processes combined with the genotoxicity of nZVI in the end leads to cell death.

The nZVI as a strong reducing agent interacts with the cell membrane and makes it more permeable, therefore potentially leading to imbalances in the homeostatic systems of plants. This closely relates to the exposure time, where the longer exposure leads to changes in the root cell membranes, essentially destroying and deforming them, leading to defective permeability and potential excessive concentrations of nutrients within the plants (Cui et al., 2023).

In the study by Gil-Díaz et al. (2024), they discovered that lettuce plants grown and treated with nZVI showed some morphological changes in their roots. While there were no changes in the cells of lettuce root cells grown in the acidic soil, alkaline soil-grown lettuce root cells showed less organelles and greater disorganization. There was traced iron homogeneously distributed in the root cells of control plants, while the nZVI-treated lettuce roots had deposits of iron in the cell walls, cytoplasm, and mitochondria, regardless of the soil pH.

According to the study by Sun et al. (2019), mung bean plants TEM imaging showed plasmolysis, breakage of cytomembrane, multiple nuclei, and contracted cytoplasm in the root cells after exposure to starch stabilized nZVI. The roots had nZVI plaque on the outside of the roots, with some of nZVI also penetrating the cell wall.

As part of the discussion on the cellular functions of plants it is inevitable to mention photosynthesis. The process of photosynthesis can be described as a conversion of light energy to chemical energy in the form of ATP, NADH and NADPH molecules that can be utilized by organisms, such as plants, which use them to facilitate carbon dioxide fixation and produce sugars with release of oxygen as a byproduct (Bowyer & Leegood, 1997).

It is important to investigate the effects of nZVI on photosynthesis, whether it can increase it, therefore induce plant growth and promote nutrient uptake. Taking these factors into account, it can potentially be of great use as a fertilizer and carbon dioxide uptake promotor (Yoon et al., 2019).

Another aspect to consider is the nZVI effect on the stress that potentially risky metals induce in plants, in this context, on the photosynthetic functions and related. Findings by Anwar et al. (2024) led to a conclusion that nZVI greatly influences chlorophyll synthesis and significantly counteracts Cd toxicity. In view of these factors, Cd stress on tomato seedlings negatively influences chlorophyll synthesis. Due to the Cd stress, chlorophyll a was reduced by 23.86% and chlorophyll b by 14.84%, while the addition of nZVI enhanced chlorophyll a by 25.99% and chlorophyll b by 16.10%.

The nZVI concentration is a great factor in many processes, including photosynthesis. Wang et al. (2016) reported that at 1000 mg kg^{-1} of nZVI, carotenoid pigments and chlorophyll pigments were suppressed greatly, leading to reduced photosynthesis and lower biomass in rice seedlings. While in another study, Kim et al. (2019) noted an increase in chlorophyll concentrations in a crop plant *Medicago sativa* (alfalfa) grown in soil treated with a very small concentration of nZVI. Based on these studies, it is reasonable to conclude that photosynthesis is dependent on nZVI concentration, and nZVI effects on photosynthesis are also dependent on plant species. Yoon et al. (2019) recorded that nZVI also supported stomatal openings of the *Arabidopsis thaliana* plant, therefore increasing photosynthesis and promoting plant growth as well. Plant´s content of nutrients, starch, iron and soluble sugars was also increased.

3.5.5 nZVI´s stress responses in plants

The nZVI has been noted to impact phenotypic changes in plants, but the observable changes vary, such as chlorosis, usually on the nZVI type and concentration or plant species. Phenotypic changes observed in cattail (*Typha latifolia*) in the study by Ma et al. (2013) were at nZVI levels over 200 mg L^{-1}. Compared to the control samples, the treated plants, after four weeks, showed signs of stunted growth, lower biomass, and dry leaves. The changes in root morphology were also noted; the roots appeared much darker due to the nZVI and iron oxide accumulation on their surface. Further transport into the cells of plants by the root tips was not noted in *Typha*, but noted in the hybrid poplars (*Populous deltoids* × *Populous nigra*), probably due to structural differences of monocots, with higher amounts of lignin, and dicots. Issue

arising from accumulation on the outside of the roots, is the alteration of nutrient and water uptake of plants. Based on the findings of Sun et al. (2019), changes in the leaf colour of seedlings of mung bean (*Vigna radiata*) started on day four of starch stabilized nZVI exposure, and by day nine, the symptoms worsened, and the blackened leaves started to fall off. While, unlike in the case of starch stabilized nZVI, the bare nZVI exposure had no toxic effects on the mung bean, showcasing the nZVI type influence. The nZVI also affects the plant´s shoot phenotype. A study on the *Arabidopsis thaliana* shoots showed a clear difference between nZVI-treated and nontreated shoots. The shoots treated with nZVI had 38% larger leaves and 38% larger dry weight of their rosette than the nontreated, meaning nZVI supported shoot growth (Yoon et al., 2019).

Oxidative stress and lipid peroxidation of the membranes in plants are measured by malondialdehyde concentration, while free radical removal is measured in catalase, peroxidase, and superoxide dismutase concentration as they are the responsible enzymes. It is noted that, on average, malondialdehyde, catalase and peroxidase activity usually does not change after nZVI application, but superoxide dismutase, on average, increases after application, therefore the physiological response in reactive oxygen species removal in plants can be affected (Cui et al., 2023).

Anwar et al. (2024) measured enzymatic activity and production of reactive oxygen species after Cd exposure from the tomato seedlings. Enzymes that are responsible for a plant´s defence system in case of a present stressor, such as Cd, are peroxidase, glutathione, ascorbate peroxidase, catalase, and superoxide dismutase. Purely Cd spiked seedlings showed a decrease in enzymatic activity, while nZVI treated Cd spiked group showed increased enzymatic activity, though still lower than the control group. Number of oxygen reactive species, H_2O_2 and O_2^-, and malondialdehyde concentration rose in Cd spiked groups, but decreased in nZVI treated Cd spiked soil. Therefore, they concluded that nZVI potentially triggers a defence mechanism against Cd stress, and reduces production of reactive oxygen species.

Above mentioned enzymes also work with non-enzymatic molecules such as proline, glutathione, flavonoids, ascorbate, α-tocopherol, phenolics, carotenoids, to contribute to plant defence system, and reduce stress induced oxidative damage (Zandi & Schnug, 2022; Li et al., 2021a). Despite the lack in research examples of non-

enzymatic responses induced by nZVI, there are a couple of instances that can be found. In the study by Mielcarz-Skalska et al. (2021), they observed changes in the non-enzymatic cell metabolites, flavonoids and polyphenols in *Lolium westerwoldicum* impacted by nZVI treatment. Flavonoid content was overall decreased by 30%, except in the case of 0.5 g of bare nZVI, which showed an increase in flavonoids in the plants leaves. Regarding roots, the flavonoid content was increased in case of bare and PAA-coated nZVI. On the other hand, the polyphenol content in the roots showed a 200% increase in the case of both types of nZVI mentioned. The high polyphenol content may improve the remediation of soil contaminants, as polyphenols have the ability to prevent aggregation of iron. Another example is the high dose of nZVI that triggered proline content by 3% as a stress response, alongside chlorophyll a and b by 14% and, as a response to lipid peroxidation, malondialdehyde by 97% in white willow (*Salix alba* L.) (Mokarram-Kashtiban et al., 2019).

As mentioned before, many plant functions are dependent on nZVI concentration. Conversely to a negative response of white willow at a high nZVI dose, nZVI at a low dose of 50 mg kg^{-1} disrupted the metabolic pathways in maize (*Zea mays* L.) roots compared to no changes found at the higher dose of 500 mg kg^{-1}. The changes in the metabolic pathways, more specifically their activation, could potentially benefit the plant and improve its response to various stressors. The processes that nZVI altered encompassed arginine biosynthesis and aminoacyl-tRNA biosynthesis; metabolism of alanine, aspartate, and glutamate; arginine and proline metabolism; butanoate metabolism; glutathione metabolism; glyoxylate and dicarboxylate; and pyrimidine metabolism (Wang et al., 2021b).

4 Experimental part

4.1 Methodology

4.1.1 Assessment of the analysed soil and amendments

The soil used for the experiments was collected from the area of a smelter in the Czech Republic from the top (0-20 cm) soil layer. The soil was classified as Technosol, as it originated as a mixture of soil, various wastes and organic debris from the smelter area. The soil samples collected were air-dried and sieved through a 2 mm steel mesh sieve. Sulphidated nZVI (marked further in text as nZVI for simplification;

commercial product Nanofer 25DS) was purchased from Nano Iron, s.r.o., Czech Republic. Thermally treated (dried at 90°C) sewage sludge was obtained from a small wastewater treatment plant in the Czech Republic. The sludge and the soil samples were digested under microwave conditions (Multiwave PRO, Anton Paar, Austria) following the US EPA method 3051A. Specifically, 0.5 g of sample was digested in a mixture of HNO_3, HCl and HF in a ratio 9:3:1. Following the microwave acid digestion, the samples were evaporated to dryness at 100°C and dissolved in 10 mL of 2% HNO_3 solution. Certified reference materials BCR-483 and NIST 2710A were used for quality control. The total elemental concentrations in the soil and sludge were assessed after the acid digestion using the inductively coupled plasma optical emission spectrometry (ICP-OES; Thermo Scientific iCAP 7000 Plus Series).

4.1.2 Experimental setup of the incubation period

The 60 plastic planters with the dimensions of 14 cm in height and 20 cm in width were filled with 1 kg of the amended or non-amended (control) soil. The soil was prepared in six different ways: control, 1% nZVI (w/w), 2% nZVI (w/w), 3% Sludge (w/w), 3% Sludge (w/w) + 1% nZVI (w/w), and 3% Sludge (w/w) + 2% nZVI (w/w). Each variant was performed in 5 replicates. The plant species selected for the experiment were *Festuca rubra* (FR) and *Arrhenatherum elatius* (AE), based on the pilot study used to determine the best phytostabilisation candidates. To equilibrate the soil prior to seeds planting, it was kept in the greenhouse for 8 weeks and watered to about 70% field capacity. The seeds were planted to a depth of 1.5 to 2.0 cm and regularly watered twice a week. The pots were kept for 60 days under the greenhouse conditions: a temperature range between 20-25°C, 12 hours daylight/12 hours darkness, photosynthetically active radiation 225 µE m^{-2} s^{-1}, humidity of 60-80%. After the 60-day incubation period, the grown plants were harvested and separated into shoots and roots. Shoots biomass and length were measured. Roots and shoots obtained from both plant species were then thoroughly washed and rinsed with distilled water, dried at room temperature, and oven-dried at 60° C for 48 h to obtain the dry weight of the biomass and be ready for further digestion.

4.1.3 Determination of total elemental concentration in roots and shoots of the plants

Following the drying of the roots and shoots of the plants, they were milled in a mechanical grinder or ground with mortar and pestle to prepare the samples for digestion. The digestion was done using a modified plant digestion procedure by Zinzala et al. (2023). Specifically, 0.25 g of the roots and shoots samples were microwave digested using 5 mL HNO_3 and 1 mL H_2O_2 and subsequently evaporated to dryness at 100° C. The dried samples were dissolved in 10 mL of 2% HNO_3 solution. Certified reference material ERM-CD281 RYE GRASS was used to assess the quality of the sample digestion via a comparison of the results obtained for the certified values. The digested samples were filtered through a 0.45 μm cellulose acetate filter and further analyzed for the total elemental concentration determination using ICP-OES.

4.1.4 pH and Eh determination and soil extraction

Following the plant harvest, pH and soil extraction analyses were done to determine the impact of the amendments on the soil parameters. The active pH of the soil was measured in a suspension using a 1:2.5 (w/v) ratio of soil/deionized water, while the exchangeable pH was measured in a suspension using 1 M KCl (ISO 10390:1994). Soil water extraction was done using deionized water following the procedure by Mitzia et al. (2019). Specifically, 4 g of dried soil was mixed with deionized water in a ratio of 1:10 (w/v). The containers with the extraction mixture were then shaken for 3 h (200 rpm) and centrifuged for 10 min at 9000 rpm. The supernatant was filtered through a 0.45 μm cellulose acetate syringe filter, and the Eh (ORP electrode SenTix ORP 900, WTW) and pH (inoLab® pH metre; pH 7310, WTW, Germany) in the filtrate were determined. The content of the metals in the filtrate was determined using ICP-OES.

4.1.5 Statistical evaluation

Statistically significant differences between different treatments were determined for the pH data, plant height, biomass yield and contents of the main contaminants (As, Cd, Pb and Zn) in the soil water extracts and plant shoots and roots. The analysis of variance (one-way ANOVA) at $P < 0.05$, with a subsequent Tukey test when appropriate were performed using SigmaPlot 14.0 (Systat Software Inc., USA).

4.2 Results

4.2.1 Initial characterisation of soil

Table 2 presents values of different elemental concentrations in soil with different amendments prior to planting of *Festuca rubra* (FR) and *Arrhenatherum elatius* (AE). The table provides an insight into changes of elemental concentrations from the control soil when 1% nZVI and 2% nZVI, 3% sludge, and a combination of 1% nZVI and 2% nZVI and 3% sludge were mixed into the soil. Notable changes occurred in regard to Fe for all amendments. Other notable changes occurred in K and Na in 1% nZVI and 2% nZVI. Ca, Mn, P, Na, and Zn were affected by the 3% sludge. 1% nZVI + 3% sludge and 2% nZVI + 3% sludge show comparable changes to 1% nZVI, 2% nZVI, and 3% sludge, respectively.

Table 1Ministry of the Environment of the Czech Republic (Act No. 437/2016) - Limit concentrations of metals and metalloids in agricultural soils measured in aqua regia extract (just Hg is determined after total digestion) in mg/kg in soil

	As	Cd	Cr	Cu	Hg	Ni	Pb	Zn	Be	Co	V
Normal soils	20	0.5	90	60	0.3	50	60	120	2	30	130
Light soils	15	0.4	55	45	0.3	45	55	105	1.5	20	120

Although the Technosol used in the experiment does not belong to the category of agricultural soil, concentrations of potentially risky elements were compared for basic orientation with the limit values of these elements in the agricultural soils set by the Ministry of the Environment of the Czech Republic in Table 2. For both normal and light soil the elements exceeding the limit throughout all amendments are As, Cd , Cu, Ni, Pb and Zn, while Cr exceeds the limits only in 1% nZVI + 3% sludge and 2% nZVI + 3% sludge. From these elements, As, Cd, Pb and Zn were identified as the main contaminating elements, exceeding the limit values by the orders of magnitude. This metal(loid)s were also the main focus the tested remediation using nZVI and sludge.

Table 2 Mean values of initial soil element concentrations (mg/kg) with corresponding standard deviation across different soil amendments.

	Control	1% nZVI	2% nZVI	3% Sludge	1% nZVI + 3% Sludge	2% nZVI + 3% Sludge
As	348 ± 41	313 ± 16	234 ± 94	315 ± 26	285 ± 33	278 ± 33
Ca	11391 ± 246	10942 ± 807	12879 ± 3992	6766 ± 3696	6626 ± 2018	7919 ± 4329
Cd	47 ± 3	46 ± 2	45 ± 6	40 ± 3	35 ± 1	34 ± 2
Cr	68 ± 2	76 ± 2	79 ± 3	78 ± 15	90 ± 2	113 ± 2
Cu	703 ± 21	720 ± 11	700 ± 27	680 ± 25	652 ± 22	722 ± 37
Fe	41442 ± 1048	51550 ± 2976	54315 ± 337	36072 ± 2878	39456 ± 3063	47430 ± 2454
K	5070 ± 753	5048 ± 447	4538 ± 384	4662 ± 438	4556 ± 253	4739 ± 486
Mg	1493 ± 189	1544 ± 560	1220 ± 34	676 ± 519	432 ± 94	503 ± 252
Mn	1877 ± 113	1805 ± 56	2019 ± 699	1788 ± 179	1633 ± 86	1642 ± 64
Na	3329 ± 66	3445 ± 219	3097 ± 157	2784 ± 301	2720 ± 145	2806 ± 329
Ni	56 ± 3	61 ± 5	61 ± 7	57 ± 7	53 ± 1	58 ± 0
P	983 ± 23	962 ± 49	821 ± 255	1299 ± 86	2507 ± 75	1847 ± 147
Pb	9073 ± 750	8971 ± 778	9576 ± 957	6912 ± 530	6821 ± 510	7037 ± 409
S	2121 ± 148	2408 ± 256	2244 ± 236	2020 ± 178	2642 ± 65	2415 ± 41
Zn	5608 ± 60	5673 ± 181	5279 ± 586	4790 ± 425	5108 ± 380	4966 ± 196

4.2.2 Soil active and exchangeable pH

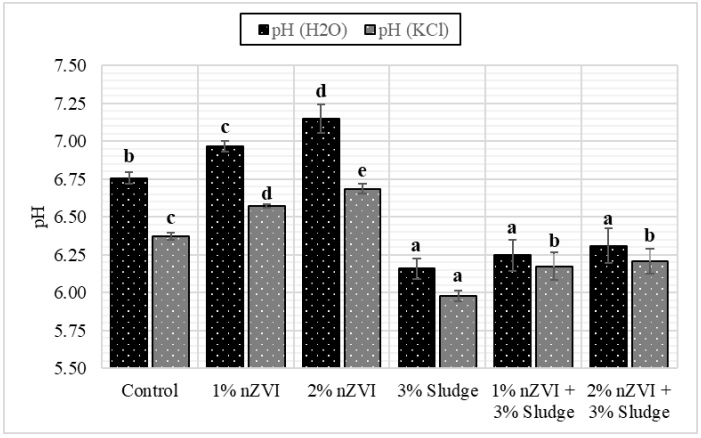

Fig. 1 Mean values of active and exchangeable acidity and the corresponding standard deviations of soil pH after AE cultivation. The statistical analysis was performed separately for each type of pH measured. Data with different letters indicates statistically significantly different values (P<0.05).

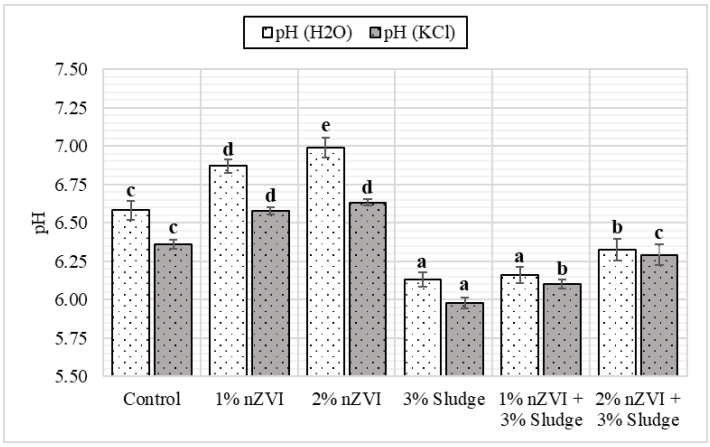

Fig. 2 Mean values of active and exchangeable acidity and the corresponding standard deviations of soil pH after FR cultivation. The statistical analysis was performed separately for each type of pH measured. Data with different letters indicates statistically significantly different values (P<0.05).

Graphs in Fig. 1 and Fig. 2 illustrate the pH levels across control soil and amended soils which were measured after *Arrhenatherum elatius* (AE) and *Festuca rubra* (FR) were harvested. Generally, the pH values compared between both grass species showed very similar values. A notable change in pH compared to the control soil pH is the increase across 1% nZVI and 2% nZVI, reaching neutral and alkaline values. Acidification across 3% sludge, 1% nZVI +3% sludge and 2% nZVI + 3% sludge amendments can be noted, the trend following the addition of 1% nZVI and 2% nZVI can be comparably seen in the samples including sludge. The sludge thus showed its tendency to decrease the soil pH, while nZVI promoted the pH increase.

4.2.3 Extraction of soil with deionized water

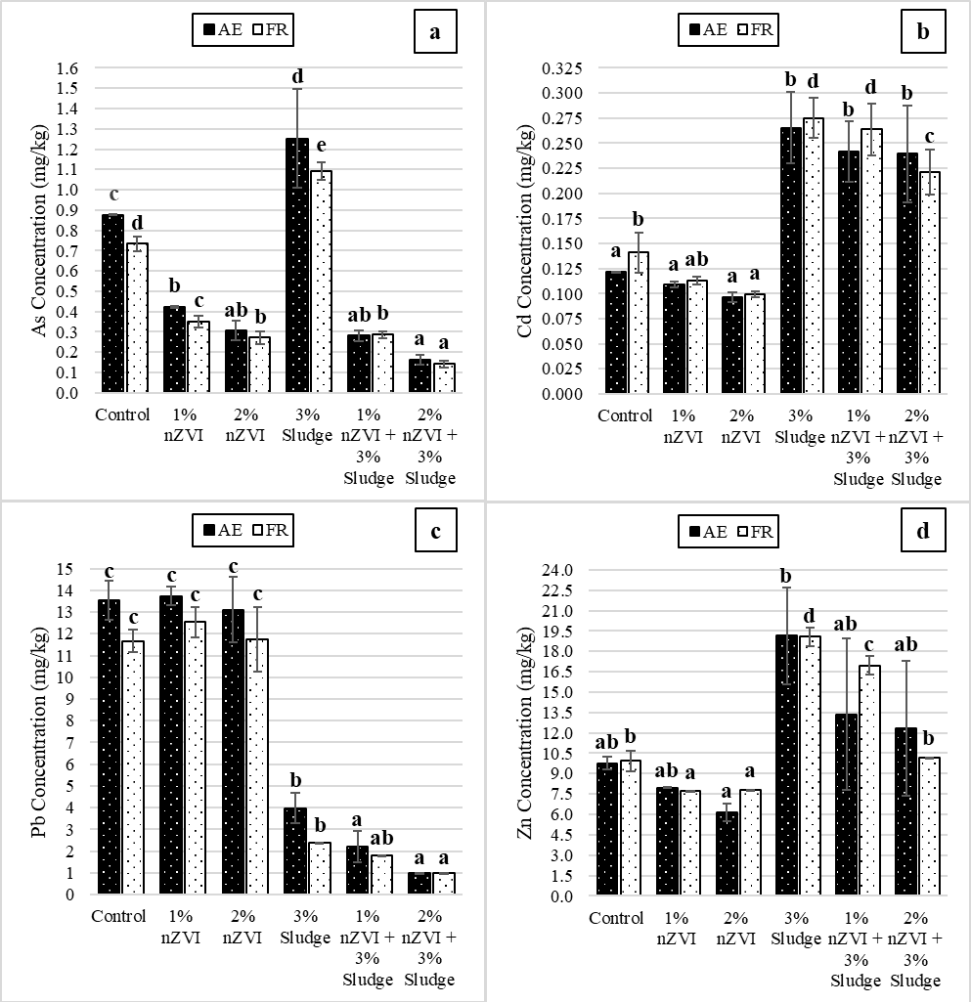

Fig. 3 Mean concentrations of As (a), Cd (b), Pb (c), and Zn (d) in the soil water extract after AE and FE harvest and their corresponding standard deviation values. The statistical analysis was performed separately for AE and FE. Data with different letters indicates statistically significantly different values ($P<0.05$).

Fig. 3 shows comparative levels of As, Cd, Pb, and Zn concentrations in the soil water extract following AE and FE harvest. Fig. 4a depicts increased As levels in control and 3% sludge samples, while 1% nZVI, 2% nZVI, 1% nZVI + 3% sludge, and 2% nZVI + 3% sludge show a decrease compared to the control sample. Fig. 3b depicts almost double the levels of Cd in 3% sludge, 1% nZVI + 3% sludge, and 2% nZVI + 3% sludge. Fig. 4c depicts similarly high Pb concentrations in control, 1% nZVI, and 2% nZVI compared to more than three times lower Pb concentration in 3% sludge, 1% nZVI + 3% sludge, and 2% nZVI + 3% sludge. Lastly, Fig. 3c depicts Zn concentrations to follow a similar trend as Cd concentrations in Fig. 3b.

Table 3 Mean values of other elements in the soil water extract collected after AE cultivation determined using ICP-OES and their corresponding standard deviation values.

	Control	1% nZVI	2% nZVI	3% Sludge	1% nZVI + 3% Sludge	2% nZVI + 3% Sludge
Ca	216.82 ± 10.94	180.4 ± 6.77	145.35 ± 17.41	822.13 ± 138.17	769.9 ± 237.59	917.69 ± 173.3
Cr	0.09 ± 0	0.09 ± 0	0.09 ± 0.01	0.03 ± 0	0.04 ± 0.02	0.03 ± 0
Cu	1.79 ± 0.45	1.99 ± 0.01	1.99 ± 0.01	1.4 ± 0	1 ± 0	1 ± 0
Fe	8.17 ± 0.84	12.54 ± 0.52	14.7 ± 3.62	1.99 ± 0.7	1.8 ± 2.12	1.59 ± 0
K	106.01 ± 10.25	78.65 ± 2.56	97.68 ± 4.33	223.59 ± 43.62	228.99 ± 25.26	254.24 ± 20.06
Mg	28.4 ± 1.53	23 ± 0.52	19.36 ± 2.7	116.09 ± 17.92	109.2 ± 30.62	124.57 ± 19.2
Mn	1 ± 0	1 ± 0.01	0.99 ± 0.01	5.78 ± 1.42	6.78 ± 3.49	7.97 ± 2.13
Na	21.82 ± 3.33	88.51 ± 3.99	178.18 ± 15.06	54.11 ± 5.78	146.51 ± 13.55	259.67 ± 8.76
Ni	0.26 ± 0.04	0.07 ± 0	0.08 ± 0.01	0.12 ± 0.03	0.11 ± 0.02	0.12 ± 0.02
P	4.98 ± 0.01	2.99 ± 0.02	2.98 ± 0.02	11.76 ± 0.03	2.99 ± 0.01	1.99 ± 0
S	40.66 ± 3	83.04 ± 3.32	150.46 ± 20.13	134.54 ± 9.5	169.54 ± 11.33	228.52 ± 6.8

Table 4 Mean values of other elements in the soil water extract collected after FE cultivation determined using ICP-OES and their corresponding standard deviation values.

	Control	1% nZVI	2% nZVI	3% Sludge	1% nZVI + 3% Sludge	2% nZVI + 3% Sludge
Ca	322.92 ± 45.26	241.57 ± 14.07	250.03 ± 107.2	862 ± 82.04	894.21 ± 10.88	802.69 ± 29.38
Cr	0.09 ± 0.02	0.09 ± 0	0.08 ± 0	0.03 ± 0	0.03 ± 0	0.03 ± 0
Cu	1.49 ± 0.58	1.19 ± 0.7	1.19 ± 0.71	0.99 ± 0	1 ± 0	0.99 ± 0
Fe	5.21 ± 0.52	9.55 ± 1.41	11.36 ± 4.27	1.19 ± 0.71	1.6 ± 0.71	1.79 ± 0.7
K	187.79 ± 11.41	146.63 ± 19.69	158.25 ± 30.56	285.17 ± 1.98	324.22 ± 4.52	305.32 ± 20.5
Mg	43.8 ± 6.04	31.74 ± 2.11	29.95 ± 12.43	127.18 ± 14.42	125.34 ± 1.96	113.23 ± 3.79
Mn	0.99 ± 0	0.99 ± 0	1 ± 0.01	8.34 ± 2.08	8.38 ± 0.01	8.55 ± 2.1
Na	23.22 ± 1.2	97.01 ± 0.71	179.27 ± 26.96	55.89 ± 8.29	151.85 ± 4.04	243 ± 4.05
Ni	0.1 ± 0.05	0.07 ± 0	0.07 ± 0	0.11 ± 0.01	0.11 ± 0.01	0.11 ± 0.01
P	3.97 ± 0.02	2.59 ± 0	2.59 ± 0.71	10.52 ± 0.03	2.99 ± 0	1.99 ± 0
S	52.35 ± 3.36	86.17 ± 7.03	130.41 ± 25.16	149.33 ± 22.1	167.27 ± 1.92	221.62 ± 0.24

Table 3 and Table 4 show other elements present in water extract. Fe shows an increase in concentration in correlation to 1% nZVI and 2% nZVI amendments. Ca, K, Mg, and S showed a significant increase in their concentrations throughout the 3% Sludge, 1% nZVI + 3% Sludge and 2% nZVI + 3% Sludge. P shows a spike in the 3% Sludge amendment in both Table 3 and Table 4, but remains relatively similar among the control and other 4 amendments.

4.2.4 Plant biomass (dry and wet weights of shoots and roots)

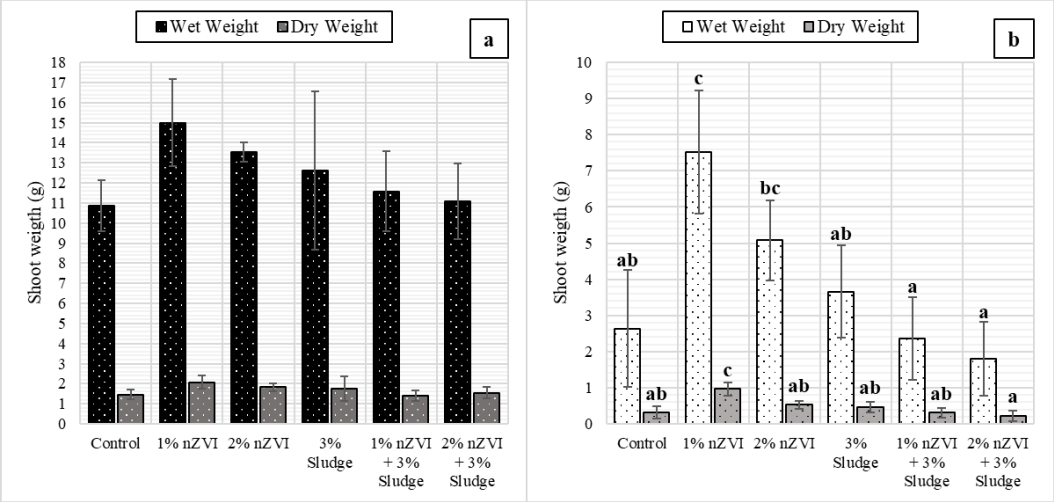

Fig. 4 Mean values of shoot weights before and after drying for plants AE (a) and FR (b) and their corresponding standard deviation values. The statistical analysis was performed separately for wet and dry weight. Data with different letters indicates statistically significantly different values (P<0.05), conversely, data with no letters indicates so statistically significant differences.

Fig. 4a and Fig. 4b depict the weights (g) of the shoots of AE and FR cultivated in different soil amendments, respectively, before and after drying. In both figures, there was a spike in the wet and dry weights of the shoots in the 1% nZVI amendment compared to the control soil and other amendments. Fig. 4b shows the 1% nZVI + 3% Sludge and 2% nZVI + 3% Sludge amendments had lesser wet and dry weights than that of the control group, and Fig. 4a shows a lesser dry weight in 1% nZVI + Sludge than the control. The average wet weight of the shoots was 12.44 g and 3.84 g in Fig. 4a and Fig. 4b, respectively. The average dry weight of the shoots was 1.68 g and 0.47 g in Fig. 4a and Fig. 4b respectively.

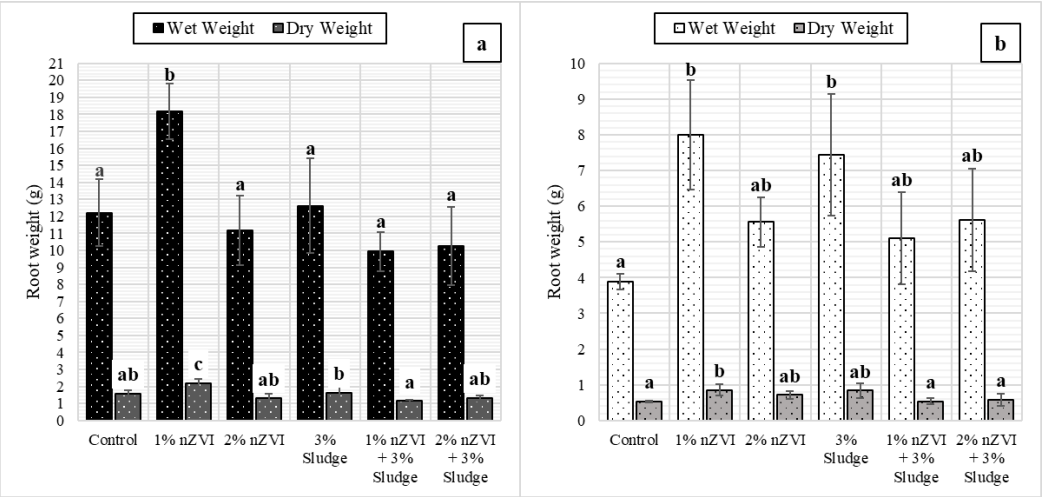

Fig. 5 *Mean values of root weights before and after drying for plants AE (a) and FR (b) and their corresponding standard deviation values. The statistical analysis was performed separately for wet and dry weight. Data with different letters indicates statistically significantly different values (P<0.05).*

Fig. 5a and Fig. 5b show the wet and dry weights (g) of the roots of AE and FR plants cultivated in different soil amendments, respectively. In Fig. 5a, there was a spike in the wet and dry weights of 1% nZVI, and in Fig. 5b, there was a spike in 1% nZVI and 3% Sludge. There was also a slight increase in the wet and dry weights in the 3% Sludge and 2% nZVI + 3% Sludge in Fig. 5a, and a slight increase in the wet and dry weights of 2% nZVI + 3% Sludge in Fig. 5b. The average wet weights in Fig. 5a and Fig. 5b were 12.40 g and 8.89 g respectively, and the dry weights were 1.53 g and 1.06 g respectively.

4.2.5 Plant height

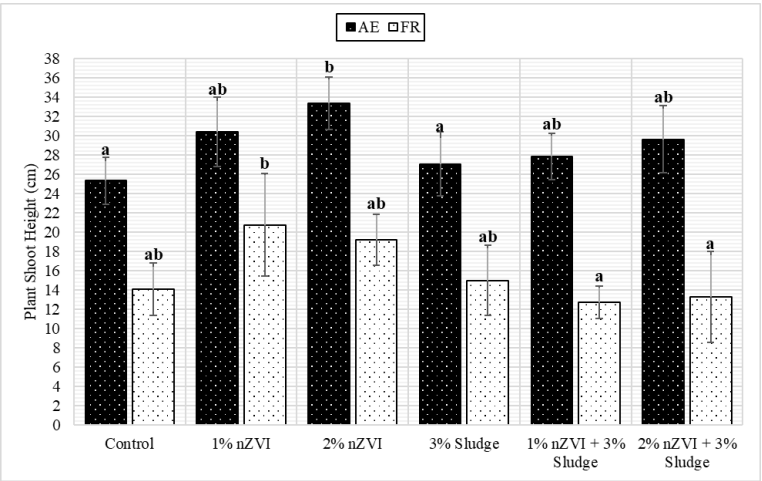

Fig. 6 Shoot heights of FR and AE after the harvest and their corresponding standard deviation values. The statistical analysis was performed separately for AE and FE. Data with different letters indicates statistically significantly different values (P<0.05).

The bar graph in Fig 6. describes the differences in shoot heights (cm) of AE and FR grown in different soil amendments. Plant AE shows on average higher shoot heights compared to the average shoot heights of plant FR. The highest shoot heights in AE are represented in the 2% nZVI amended soil sample, while in FR are represented in the 1% nZVI amended soil sample. The lowest shoot height of AE is shown in the control sample, while in FR it is shown in the 1% nZVI + 3% sludge soil amended sample.

4.2.6 Plant digestion

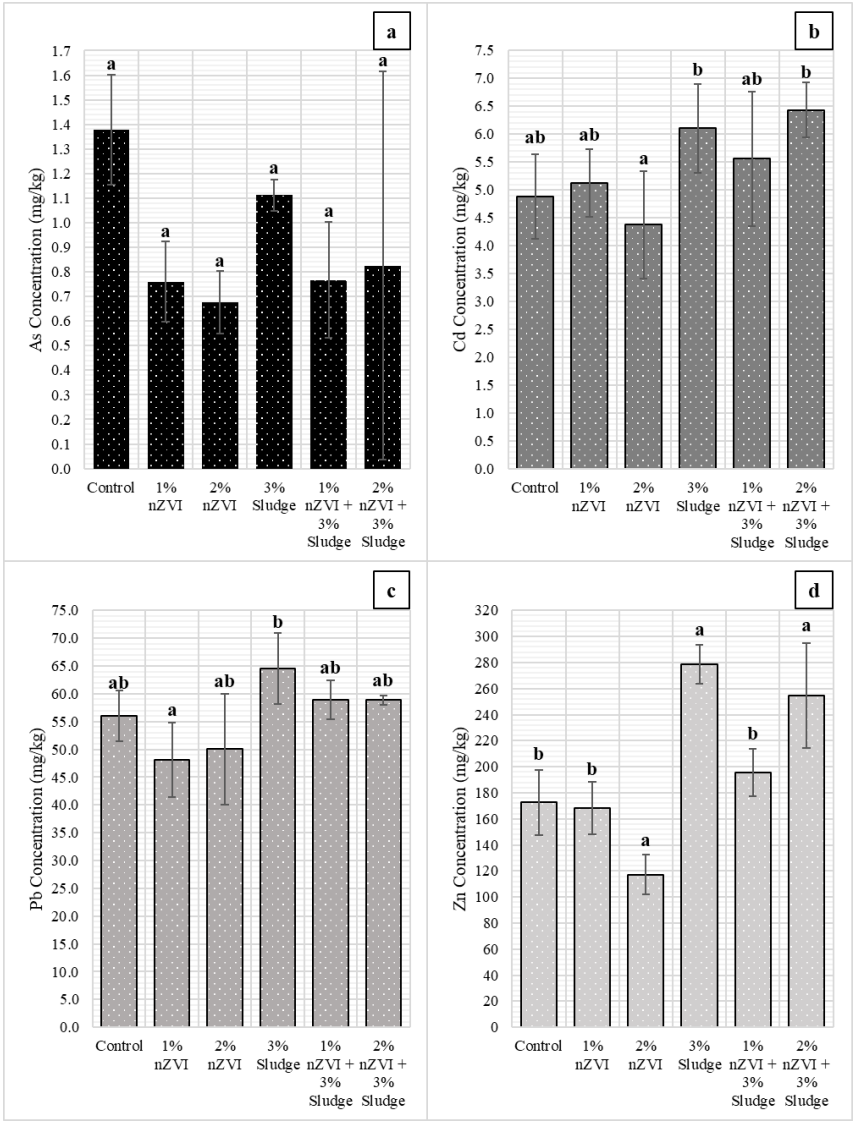

Fig. 7 Mean concentrations of As (a), Cd (b), Pb (c), and Zn (d) in shoots of AE and their corresponding standard deviation values. Data with different letters indicates statistically significantly different values ($P<0.05$).

Fig. 7 depicts the concentrations of: a) As, b) Cd, c) Pb, d) Zn in AE shoot biomass. Fig. 7a shows As concentrations were highest 3% Sludge amended soil, while the 1% nZVI and 2% nZVI amended soil showed the lowest concentrations. In Fig. 7b, Cd concentrations were highest in 2% nZVI + Sludge and 3% Sludge amended soil, while the two lowest concentrations were in the control and 2% nZVI soil amendment, with a slight increase from the control to the 1% nZVI amendment. Fig. 7c depicts the highest Pb concentration in the 3% Sludge amended soil, while the other soil amendments fluctuate in Pb concentration. Fig. 7d shows the two highest Zn concentrations in the 3% Sludge and 2% nZVI + 3% Sludge amended soil, while the lowest concentration was in the 2% nZVI amended soil.

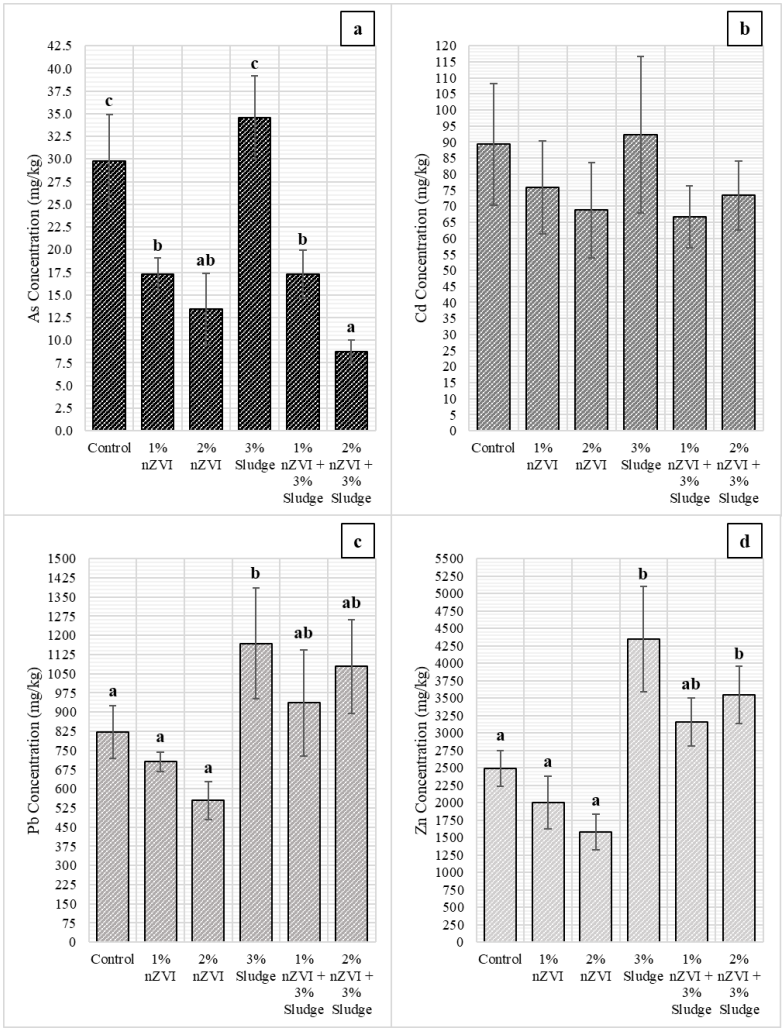

Fig. 8 Mean concentrations of As (a), Cd (b), Pb (c), and Zn (d) in roots of AE and their corresponding standard deviation values. Data with different letters indicates statistically significantly different values ($P<0.05$), conversely, data with no letters indicates so statistically significant differences.

Fig. 8 depicts the concentrations of: a) As, b) Cd, c) Pb, d) Zn in AE root biomass. In Fig. 8a, As concentrations in roots decreased with the introduction of nZVI in all nZVI amended variants, with the highest concentration in the 3% Sludge variant, and the lowest in the 2% nZVI + 3% Sludge variant. Fig. 8b depicts a decrease in Cd concentrations in the 1% nZVI, 2% nZVI, and 1% nZVI +3% Sludge amended soil, but an increase in 2% nZVI + 3% Sludge amended soil. The highest Cd concentration was in the 3% Sludge amended soil, and the lowest was in the 1% nZVI + 3% Sludge amended soil. As highlighted in Fig. 8c, the highest Pb concentrations were in the 3% Sludge and 2% nZVI + 3% Sludge amended soil, while the lowest concentration was in the 2% nZVI amended soil. Fig. 8d shows similarity to the Zn concentrations shown in Fig. 10d, with the highest concentrations in the 3% Sludge and 2% nZVI + 3% Sludge amended soil, and the lowest in the 2% nZVI amendment.

Table 5 and Table 6 present the mean elemental concentrations (mg/kg) present in the AE shoots and roots, respectively, that were not depicted by the graphs in Fig. 7 or Fig. 8. As depicted in Table 5, Mn concentration in the AE shoots increased throughout the different soil amendments, whereas the other elements show similar patterns to the concentrations depicted in the graphs of Fig. 7. There was one outlier in Table 5, which is the low concentration of P in the 1% nZVI amendment, but there was a decrease of Fe concentration from the 1% nZVI to the 2% nZVI amendment. Table 6 shows a similar decrease in Fe concentration from the 1% nZVI to 2% nZVI amendment. Table 6 also depicts similar trends to the elements depicted in the graphs in Fig. 8, and has the same outlier of the P concentration in the 1% nZVI amendment.

Table 5 Concentrations of chosen elements in AE shoots and their corresponding standard deviation values.

	Control	1% nZVI	2% nZVI	3% Sludge	1% nZVI + 3% Sludge	2% nZVI + 3% Sludge
Ca	8944 ± 1222	7058 ± 746	4892 ± 535	17706 ± 1893	14045 ± 1965	15394 ± 2707
Cr	7 ± 0	7 ± 1	7 ± 1	7 ± 1	7 ± 0	1 ± 0
Cu	14 ± 1	16 ± 1	15 ± 0	13 ± 2	12 ± 1	7 ± 1
Fe	58 ± 2	88 ± 8	78 ± 2	64 ± 6	74 ± 9	75 ± 8
K	57717 ± 3882	56012 ± 1314	57974 ± 2790	59768 ± 18511	55498 ± 3085	48527 ± 3317
Mg	3421 ± 186	3273 ± 161	2395 ± 225	4694 ± 274	3517 ± 193	4109 ± 229
Mn	27 ± 10	76 ± 29	206 ± 91	556 ± 138	438 ± 84	455 ± 82
Na	207 ± 73	330 ± 47	940 ± 361	159 ± 62	1004 ± 196	1779 ± 260
Ni	7 ± 0	6 ± 0	7 ± 1	7 ± 0	8 ± 1	4 ± 0
P	2853 ± 503	55 ± 245	2458 ± 296	4654 ± 608	5256 ± 767	4370 ± 487
S	2834 ± 157	3026 ± 135	2874 ± 445	3415 ± 274	2876 ± 226	2998 ± 63

Table 6 Concentrations of chosen elements in AE roots and their corresponding standard deviation values.

	Control	1% nZVI	2% nZVI	3% Sludge	1% nZVI + 3% Sludge	2% nZVI + 3% Sludge
Ca	4647 ± 283	3815 ± 125	3693 ± 242	7011 ± 905	6385 ± 404	5836 ± 421
Cr	7 ± 1	7 ± 0	7 ± 1	6 ± 0	7 ± 1	2 ± 0
Cu	281 ± 55	224 ± 9	166 ± 31	307 ± 55	191 ± 34	154 ± 19
Fe	281 ± 225	501 ± 93	388 ± 72	158 ± 63	189 ± 39	453 ± 70
K	8227 ± 2385	8627 ± 2152	8391 ± 874	11939 ± 3688	16519 ± 5888	10008 ± 1648
Mg	1245 ± 169	1298 ± 100	1010 ± 151	2110 ± 283	1886 ± 90	1880 ± 148
Mn	55 ± 16	83 ± 23	196 ± 85	605 ± 212	716 ± 392	793 ± 223
Na	282 ± 40	810 ± 159	1168 ± 243	394 ± 56	1155 ± 227	1876 ± 366
Ni	12 ± 5	8 ± 0	9 ± 1	11 ± 1	10 ± 1	7 ± 0
P	1991 ± 362	624 ± 216	1843 ± 424	3279 ± 393	3565 ± 416	3213 ± 242
S	2751 ± 253	2516 ± 197	2186 ± 199	3563 ± 439	2860 ± 247	2779 ± 170

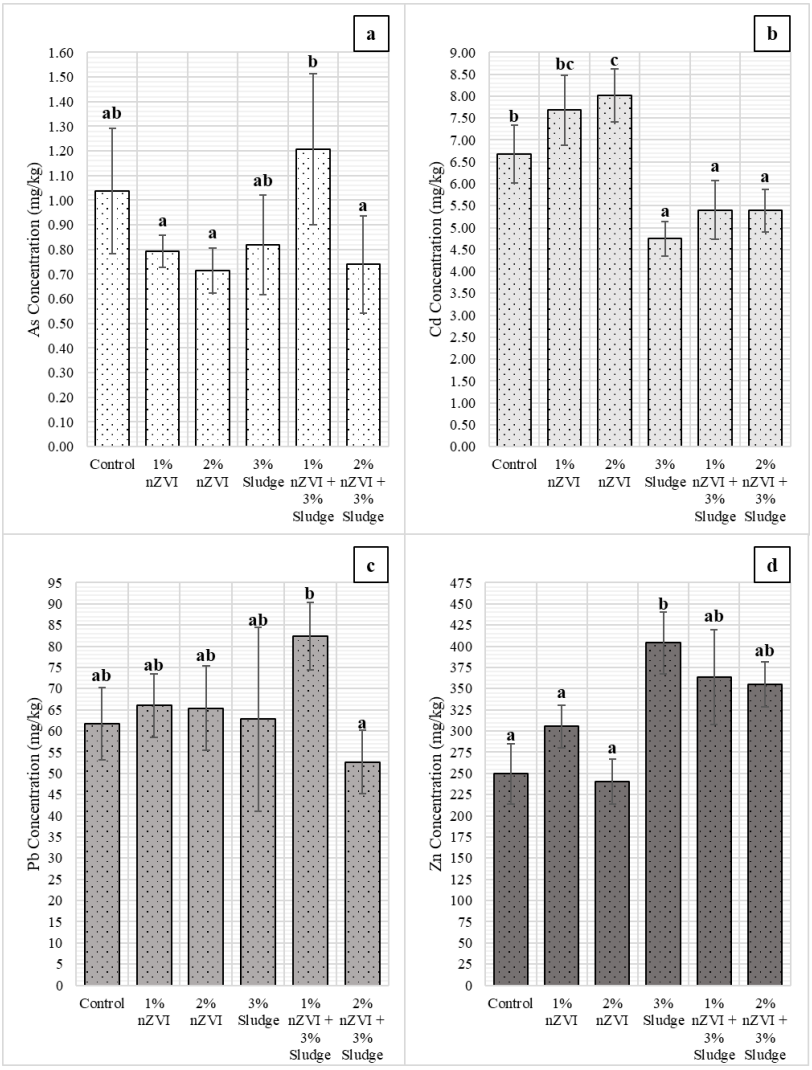

Fig. 9 Mean concentrations of As (a), Cd (b), Pb (c), and Zn (d) in shoots of FR and their corresponding standard deviation values. Data with different letters indicates statistically significantly different values (P<0.05).

Fig. 9 depicts the concentrations of: a) As, b) Cd, c) Pb, d) Zn in FR shoot biomass. Fig. 9a shows the As concentrations of FR shoots in different soil amendments, of which the control and the 1% nZVI + 3% Sludge amendment had the highest concentrations. The lowest As concentration was in the 2% nZVI amended. As seen in Fig. 9b, the Cd concentrations increased in the nZVI amended soils, with the highest concentration in the 2% nZVI amendment and the lowest in the 3% Sludge amendment. Fig. 9c depicts the Pb concentrations in FR shoots, with a steady decrease from the 1% nZVI amendment to the 2% nZVI + 3% Sludge amendment, except for a spike in the 1% nZVI + 3% Sludge amendment. In Fig. 9d, the Zn concentrations decrease from 1% nZVI to 2% nZVI regardless of sludge, but there was an increase from the control to the 1% nZVI amended soil.

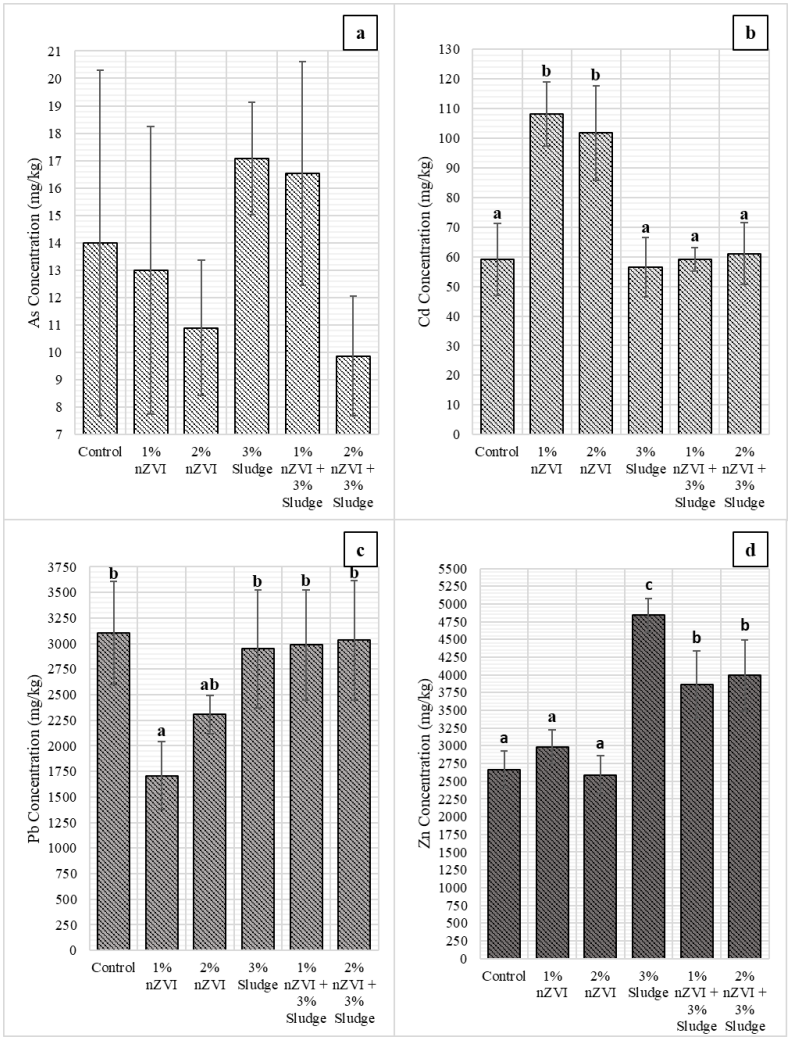

Fig. 10 Mean concentrations of As (a), Cd (b), Pb (c), and Zn (d) in roots of FR and their corresponding standard deviation values. Data with different letters indicates statistically significantly different values ($P<0.05$), conversely, data with no letters indicates so statistically significant differences.

Fig. 10 shows the concentrations of: a) As, b) Cd, c) Pb, d) Zn in FR root biomass. As depicted in Fig. 10a, the As concentration decreased in the 1% nZVI and 2% nZVI amendments with or without sludge, but there was a large drop from 1% nZVI + 3% Sludge to 2% nZVI + 3% Sludge, which was the lowest concentration. Fig. 10b shows a spike in Cd concentrations in the 1% nZVI and 2% nZVI amendments, which had the highest concentrations, and a slight increase in concentration for the 1% nZVI + 3% Sludge and 2% nZVI + 3% Sludge amendments. Fig. 10c contains the Pb concentrations in FR roots, which dropped from the control to the 1% nZVI amendment, which had the lowest concentration, which then gradually increased in the following amendments, however, the highest concentration was in the

control group. The graph in Fig. 10d shows the Zn concentrations of FR roots, which was highest in the 3% Sludge amendment, and lowest in the 2% nZVI amendment.

Table 7 and Table 8 present the mean elemental concentrations (mg/kg) of elements obtained from the ICP-OES analysis of FR shoots and roots, respectively, that were not depicted by the graphs in Fig. 9 or Fig. 10. Table 7 shows an increase in Fe concentration for 1% nZVI and 1% nZVI + 3% Sludge, but not for 2% nZVI or 2% nZVI + 3% Sludge. There were also fluctuations in the concentrations of Ca, Mg, and S across the amendments, and a spike in concentration of Mn in the 3 amendments containing 3% Sludge. The other elemental concentrations remain relatively similar across amendments. Table 8 shows and increase in Fe concentration as the percentage of nZVI increased, with the highest concentration in the 2% nZVI amendment. There was also fluctuation in the concentrations of Ca, Cu, Mg, Na, and S across the different amendments. Similar to Table 7, there was a spike in Mn concentrations in the amendments containing 3% Sludge.

Table 7 Concentrations of chosen elements in FR shoots and their corresponding standard deviation values.

	Control	1% nZVI	2% nZVI	3% Sludge	1% nZVI + 3% Sludge	2% nZVI + 3% Sludge
Ca	8215 ± 1188	6975 ± 1001	5903 ± 690	10273 ± 1679	13007 ± 2352	11221 ± 679
Cr	7 ± 0	7 ± 0	7 ± 0	2 ± 0	8 ± 2	2 ± 1
Cu	16 ± 2	19 ± 2	17 ± 1	9 ± 1	20 ± 1	9 ± 1
Fe	46 ± 10	75 ± 24	64 ± 9	63 ± 26	105 ± 25	89 ± 30
K	63227 ± 7371	63429 ± 2973	54771 ± 7562	58439 ± 10475	64808 ± 6381	58669 ± 3237
Mg	3240 ± 320	3238 ± 305	2737 ± 289	3628 ± 379	3528 ± 419	3567 ± 142
Mn	23 ± 9	48 ± 23	44 ± 16	384 ± 76	421 ± 35	382 ± 28
Na	291 ± 56	519 ± 125	1349 ± 394	447 ± 68	1171 ± 319	2061 ± 101
Ni	7 ± 1	7 ± 0	8 ± 0	4 ± 1	9 ± 1	4 ± 0
P	4997 ± 343	3850 ± 774	3729 ± 582	6696 ± 261	6843 ± 302	6174 ± 339
S	3266 ± 271	3356 ± 415	3125 ± 287	3204 ± 323	3097 ± 340	2865 ± 87

Table 8 Concentrations of chosen elements in FR roots and their corresponding standard deviation values.

	Control	1% nZVI	2% nZVI	3% Sludge	1% nZVI + 3% Sludge	2% nZVI + 3% Sludge
Ca	8795 ± 533	7035 ± 820	8656 ± 529	7496 ± 477	8617 ± 362	8424 ± 460
Cr	7 ± 0	7 ± 1	8 ± 1	2 ± 0	7 ± 1	2 ± 0
Cu	330 ± 57	229 ± 29	276 ± 19	201 ± 42	256 ± 35	176 ± 20
Fe	442 ± 135	456 ± 48	1329 ± 314	385 ± 131	605 ± 322	741 ± 217
K	3280 ± 3477	12190 ± 6560	5577 ± 1759	18994 ± 2280	18903 ± 7781	18485 ± 3700
Mg	1290 ± 205	1641 ± 246	1359 ± 218	2163 ± 117	1938 ± 394	2089 ± 67
Mn	97 ± 19	76 ± 31	135 ± 40	1516 ± 514	2042 ± 334	2059 ± 819
Na	225 ± 19	652 ± 609	560 ± 88	377 ± 22	699 ± 194	1140 ± 149
Ni	11 ± 2	9 ± 2	13 ± 0	7 ± 1	13 ± 1	9 ± 1
P	2179 ± 767	3030 ± 833	2584 ± 519	4443 ± 260	3920 ± 683	3992 ± 310
S	2500 ± 430	3364 ± 741	2608 ± 145	3646 ± 173	3591 ± 604	3434 ± 258

4.3 Discussion

The control and amended soil samples from Table 2 show notably high concentrations of potentially risky metals such as As, Cd, Cr, Cu, Ni, Pb, and Zn, which are over the limit concentrations set by the Ministry of the Environment of the Czech Republic set in the Table 2. The exceeding concentrations can be attributed by the soil collection area which is characterized as Technosol, therefore contaminated waste and debris containing soil (Huot et al., 2014).

Increase in concentration occurred in regards to Fe for 1% nZVI and 2% nZVI amendments due to zero-valent iron consisting nZVI particles. Compared to the 3% sludge amendment alone, 1% nZVI + 3% sludge and 2% nZVI + 3% sludge, again show an increase in Fe due to addition of nZVI. Gil-Díaz et al. (2020), in their study, notes the same proportional increase in Fe concentrations with addition of nZVI to the soil. Sulphidation of nZVI also contributes to a marginal increase in S among nZVI amended soil.

Fig. 3 shows comparative levels of As, Cd, Pb, and Zn concentrations in the soil water extract following the plants' harvest. Concentrations of potentially risky metals compared to the initial soil concentrations show the effectiveness of the immobilization reached by 1% nZVI, 2% nZVI, 1% nZVI + 3% sludge, and 2% nZVI + 3% sludge. Higher concentrations of As in the control samples and 3% sludge amendments when compared to the nZVI amended soil can be attributed to lack of As immobilization. Meaning, nZVI immobilized As, to some extent, via reduction and oxidation mechanisms (Ramos et al., 2009). Soil may make complexes with As, but As still has stronger affinity to bind to nZVI. Han et al. (2021.) also notes that sulphidation of nZVI helps co-precipitate As due to sulfhydryl groups serving as binding sites.

Fig. 3b and 3d both show similar trend in concentration levels of Cd and Zn, respectively. Immobilisation of Cd and Zn compared to the control group is only marginally noted in the 1% nZVI and 2% nZVI, while more mobile forms of Cd and Zn can be noted in the 3% sludge, 1% nZVI + 3% sludge and 2% nZVI + 3% sludge. Meaning some mobile forms of Cd and Zn persist in the soil after the treatment with different soil amendments and they can be more readily taken up by plants. Jiang et al. (2023) notes that sewage sludge has a potential for adsorption of Cd and Pb, possibly

through potentially risky metal forming complexes with the organic matter. Notable P increase with the sludge soil amendment is contributed by sludge being a natural source full of P (Cydzik-Kwiatowska & Nosek, 2020).

Notably, Fig. 1 and Fig. 2 which depict mean values of pH of soil for both AE and FR show higher acidity in the amendments, 3% sludge, 1% nZVI + 3% sludge, and 2% nZVI + 3% sludge. This can correlate to the higher extractability of Cd and Zn as noted from the results of soil water extracts in Fig. 3b and 3d due to their higher availability in more acidic environments (Muhammad et al., 2012). The higher extractability of Cd and Zn can contribute to the formation of complexes with the compounds found in the root exudates of plants, such as oxalic, fumaric, malic, and citric acids (Huang et al., 2021).

In regards to the results showing Pb concentrations in the soil water extract, 1% nZVI and 2% nZVI show marginal differences with the control sample concentrations, meaning nZVI amendments alone were not enough to lower the extractability of Pb. Conversely, in the amendments containing 3% sludge, 1% nZVI + 3% sludge, and 2% nZVI + 3% sludge, there is an indication of lowered extractability.

In regards to the results from Table 3 and Table 2 which depict mean values of other elements in the soil water extract collected after AE and FR, it can be observed that plant essential nutrients such as K, Na, and P differ across the amendments. K and Na values in the extract after AE cultivation and FR cultivation are higher in sludge containing amendments, which can be attributed to sludge naturally containing higher concentrations of those elements, meaning they can provide more readily available essential plant nutrients for plants to uptake (Mosquera-Losada et al., 2009). Levels of P, on the other hand, are low, especially in nZVI amended soil, compared to sludge amended soil. This finding can be attributed to P fixation in amended soil due to high levels of Fe coming from nZVI amendments (Kommana et al., 2023). Lower P availability across sludge containing amended soil can be, on the other hand, contributed by the pH, which, as results show, is out of the P availability range of 6-7 (Johan et al., 2010).

The higher pH levels, compared to the control soil, noted in 1% nZVI and 2% nZVI can be explained by oxidation of nZVI, which leads to the production of hydroxide ions and therefore increase in soil pH (Wang & Lin, 2017). On the other

hand, sludge containing amendments acidified the soil compared to the control soil, which Truter et al. (2001) also note in their study. The organic matter in sewage sludge ionizes the hydrogen ions, which leads to a decrease in pH (Alazaiza et al., 2022).

Organic matter, such as found in sewage sludge, can act as a nZVI collector and facilitate better spread of nZVI particles in the soil (Johnson et al., 2009). Conversely, the charges of humic and fulvic acids in the sludge can compete with the ones of nZVI, reducing potentially risky metals removal (Alazaiza et al., 2022).

A higher concentration of Fe in results from both plant's digestion analysis results indicates possible translocation of Fe, originating from nZVI, into the roots of plants but no further. Similar results were shown in the study by Mielcarz-Skalska et al. (2021), where they confirmed accumulation of Fe in the roots which happened due to deformation of the root cell walls. Also, the same trend was noted, with a higher weight of roots as in the results from this study.

Mean root and shoot values in both plants, AE and FR, show the highest wet weight in 1% nZVI amended soil samples which could indicate that nZVI changed the soil morphology leading to better water uptake due to potential improvement in the soil water infiltration and reduced compaction (Chen et al., 2019). The highest dry weights recorded are in both shoots and roots of both plants, AE and FR, in the 1% nZVI and 3% nZVI amended soil. The highest weight in both shoots and roots in the 1% nZVI amended soil can indicate a balanced growth of the plants in their above and below ground biomass, or conversely, as mentioned in the study by Teodoro et al. (2020), observed FR as well. They note that the higher weight of roots can also be an indicator of toxicity due to root elongation as a stress response or aggregation of nZVI by its roots. (Teodoro et al., 2020).

Regarding the higher biomass in 3% sludge amended soil, it can be deducted that the essential nutrients attributed to plant growth.

In regards to plant height, the most effective growth was recorded for AE in 2% nZVI, while for FR, it was in 1% nZVI amended soil. However, looking at the overall results, FR shoots grew lower than AE shoots. Possible aggregation of nZVI by the roots of FR, as noted before, can be the reason behind the lower growth due to the potential blocking of the cells which can lead to lower water and nutrients uptake, therefore lesser growth, or rather just the plant species difference.

Comparing recorded pH values and the heights of the shoots of plants, it can be noted that pH of the AE and shoot heights throughout all the amendments and the control sample follow the same trends, therefore it was in an optimal pH range for its growth. While, comparing the pH and shoot height of FR, it can be noted that 2% nZVI, 3% sludge, 1% nZVI + 3% sludge, and 2% nZVI + 3% sludge soil amendments might have not been the most optimal range of pH for shoot growth. Reason for that can be attributed to activation of stressors in FR. It is often noted that high concentrations of nZVI can have inhibitory effects on the plant growth (Cui et al., 2023).

Plant digestion results reflect the findings discussed previously. It can be noted that elements that were shown to be more mobile and extractable from soil water extraction analysis are also in higher concentrations in plants, respectively, meaning the availability of those potentially risky metals was indeed a contributor for plant uptake. The essential plant nutrients, Na, K, and P are also in higher concentrations in the plant digestates meaning that they were translocated into plants.

Concentrations of As in the roots and shoots of AE show to be the least prevailing compared to the Pb, which is only marginally different from the control soil sample, while Cd and Zn show higher concentrations in sludge containing amendments, which can be again contributed to the pH or complexation with organic matter.

Looking at the other elemental concentrations, it can be observed from the tables for both shoots and roots of AE, that P concentration drops in 1% nZVI and 2% nZVI, which can again be contributed to P fixation in the presence of Fe containing amendments. Increase in Fe concentrations across 1% nZVI and 2% nZVI is arguably due to plant uptake of Fe.

Compared to the AE, the concentrations of potentially risky metals follow the same trends, with the exception of Cd. Based on the Cd concentration in the shoots, it seems to be arguably less likely immobilized by nZVI and can be readily taken up by the FR. This can potentially be due to the optimal ratio of nZVI in the soil while dealing with this species of plant and sulphidation. More iron sulphide acting particles may exhibit lower reactivity for this type of contaminant (Su et al., 2019).

From the tables 7 and 8 of other element concentrations of the shoots and roots of FR, as well as AE the concentrations of essential plant nutrients K, Na, and arguably P, are increased in nZVI amended soil, meaning that nZVI potentially facilitates nutrient uptake.

5 Conclusions

To summarise the valuable study insights and findings this thesis has highlighted in the interactions of plants and nZVI in contaminated soil environment, the following can be concluded. The contaminated environment attributed to the Technosol characteristics exceeded limit concentrations of many metallic contaminants, especially of As, Cd, Pb and Zn. In aqua regia, nZVI contributed to increased concentrations of Fe due to its iron nature, and S, due to its sulphidation in 1% nZVI and 2% nZVI amended soil. Naturally, sludge contributed to increased concentrations of K, Na, and P in 3% sludge, followed by 1% nZVI + 3% sludge and 2% nZVI +3% sludge amended soil. P values evidently decreased with the 1% nZVI and 2% nZVI across all amendment, leading to a conclusion of nZVI facilitated P fixation to soil particles. Higher availability of Zn and Cd, and potential for their plant uptake comes evidently from the sludge affected pH of the soil, which naturally more acidifying, contributed to an optimal pH for their mobility. Conversely, best immobilized element is evidently As, in the 1% nZVI and 2% nZVI. 1% nZVI + 3% sludge and 2% nZVI +3% sludge amended soil samples. 1% nZVI + 3% sludge and 2% nZVI +3% sludge amended soil interchangeably contributed to increased biomass, either by nZVI immobilizing the contaminants and making the environment less toxic for plants, or sludge contributing to increased essential nutrients, therefore greater biomass. Based on that statement alone, it can be said that they do show synergistic effects in the sense of improved biomass and contaminant immobilization, even though the effectiveness of both also varies on the level of different plant species specificity.

6 List of references

Scientific Publications

Alazaiza, M. Y. D., Albahnasawi, A., Copty, N. K., Bashir, M. J. K., Nassani, D. E., Maskari, T. A., Amr, S. S. A., Abujazar, M. S. S., 2022: Nanoscale Zero-Valent Iron Application for the Treatment of Soil, Wastewater and Groundwater Contaminated with Heavy Metals: A Review. *Desalination and Water Treatment*, volume 253: 194–210. https://doi.org/10.5004/dwt.2022.28302.

Ali, H., Khan, E., Ilahi, I., 2019: Environmental Chemistry and Ecotoxicology of Hazardous Heavy Metals: Environmental Persistence, Toxicity, and Bioaccumulation. *Journal of Chemistry*, volume 2019: 6730305. https://doi.org/10.1155/2019/6730305.

Anwar, A., Wang, Y., Chen, M., Zhang, S., Wang, J., Feng, Y., Xue, Y., Zhao, M., Su, W., Chen, R., Song, S., 2024: Zero-Valent Iron (nZVI) Nanoparticles Mediate *Slerf1* Expression to Enhance Cd Stress Tolerance in Tomato. *Journal of Hazardous Materials*, volume 468: 133829. https://doi.org/10.1016/j.jhazmat.2024.133829.

Babakhani, P., Fagerlund, F., Shamsai, A., Lowry, G. V., Phenrat, T., 2015: Modified MODFLOW-Based Model for Simulating the Agglomeration and Transport of Polymer-Modified Fe Nanoparticles in Saturated Porous Media. *Environmental Science and Pollution Research International*, volume 25, issue 8: 7180–7199. https://doi.org/10.1007/s11356-015-5193-0.

Bae, S., Collins, R. N., Waite, T. D., Hanna, K., 2018: Advances in Surface Passivation of Nanoscale Zerovalent Iron: A Critical Review. *Environmental Science & Technology*, volume 52, issue 21: 12010-12025. https://doi.org/10.1021/acs.est.8b01734.

Belal, E. S., El-Ramady, H., 2016: Nanoparticles in Water, Soils and Agriculture. In: Ranjan, S., Dasgupta, N., Lichtfouse, E. (eds.): Nanoscience in Food and Agriculture 2. Springer, New York: 311-358. https://doi.org/10.1007/978-3-319-39306-3_10.

Bennett, H. H., 1947: Soil Conservation in the World Ahead. *Journal of Soil and Water Conservation*, volume 2, issue 1: 43-50.

https://archive.org/details/sim_journal-of-soil-and-water-conservation_1947-01_2_1/page/n75/mode/2up.

Bowyer, J. R. & Leegood, R. C., 1997: Photosynthesis. In: Dey, P. M. & Harborne, J. B. (eds.): Plant Biochemistry. Elsevier, Amsterdam: 49-110.

Burducea, M., Lobiuc, A., Asandulesa, M., Zaltariov, M. F., Burducea, I., Popescu, S. M., Zheljazkov, V. D., 2019: Effects of Sewage Sludge Amendments on the Growth and Physiology of Sweet Basil. *Agronomy*, volume 9, issue 9: 548. https://doi.org/10.3390/agronomy9090548.

Chekli, L., Brunetti, G., Marzouk, E. R., Maoz-Shen, A., Smith, E., Naidu, R., Shon, H. K., Lombi, E., Donner, E., 2016: Evaluating the Mobility of Polymer-Stabilised Zero-Valent Iron Nanoparticles and Their Potential to Co-Transport Contaminants in Intact Soil Cores. *Environmental Pollution*, volume 216: 636-645. https://doi.org/10.1016/j.envpol.2016.06.025.

Chen, S. S., Hsu, H. D., Li, C. W., 2005: A New Method to Produce Nanoscale Iron for Nitrate Removal. *Journal of Nanopartical Research*, volume 6: 639-647. https://doi.org/10.1007/s11051-004-6672-2.

Chen, X., Li, X., Xu, D., Yang, W., Bai, S., 2020: Application of nanoscale zero-valent iron in Cr(VI)-contaminated soil: A review. *Nanotechnology Reviews*, volume 9, issue 1: 736-750. https://doi.org/10.1515/ntrev-2020-0059.

Chen, Y. Z., Zhou, W. H., Liu, F., Yi, S., Geng, X., 2019: Microstructure and Morphological Characterization of Lead-Contaminated Clay with Nanoscale Zero-Valent Iron (nZVI) Treatment. *Engineering Geology*, volume 256: 84-92. https://doi.org/10.1016/j.enggeo.2019.05.001.

Chi, H. Y., Zhou, X. X., Wu, M. R., Shan, W. Y., Liu, J. F., Wan, J. Q., Yan, B., Liu, R., 2023: Regulating the Reaction Pathway of nZVI to Improve the Decontamination Performance Through Magnetic Spatial Confinement Effect. Journal of Hazardous Materials, volume 447: 130799. https://doi.org/10.1016/j.jhazmat.2023.130799.

Crane, R. & Scott, T. B., 2013: The Effect of Vacuum Annealing of Magnetite and Zero-Valent Iron Nanoparticles on the Removal of Aqueous Uranium. *Journal of Nanotechnology*, volume 5: 173625. http://doi.org/10.1155/2013/173625.

Cui, X., Hou, D., Tang, Y., Liu, M., Qie, H., Qian, T., Xu, R., Lin, A., Xu, X., 2023: Effects of The Application of Nanoscale Zero-Valent Iron on Plants: Meta Analysis, Mechanism, And Prospects. *Science of The Total Environment*, volume 900: 165873. https://doi.org/10.1016/j.scitotenv.2023.165873.

Cydzik-Kwiatowska, A. & Nosek, D., 2020: Biological Release of Phosphorus is More Efficient from Activated than from Aerobic Granular Sludge. *Scientific Reports*, volume 10: 11076. https://doi.org/10.1038/s41598-020-67896-5.

Ding, Y., Liu, B., Shen, X., Zhong, L., Li, X., 2013: Foam-Assisted Delivery of Nanoscale Zero Valent Iron in Porous Media. *Journal of Environmental Engineering*, volume 139, issue 9: 1206–1212. https://doi.org/10.1061/(ASCE)EE.1943-7870.0000727.

Eljamal, R., Eljamal, O., Maamoun, I., Yilmaz, G., Sugihara, Y., 2020: Enhancing the Characteristics and Reactivity of nZVI: Polymers Effect and Mechanisms. *Journal of Molecular Liquids*, volume 315: 113714. https://doi.org/10.1016/j.molliq.2020.113714.

Elliot, D. W., & Zhang, W. X., 2001: Field Assessment of Nanoscale Bimetallic Particles for Groundwater Treatment. *Environmental Science & Technology*, volume 35, issue 24: 4922-4926. https://doi.org/10.1021/es0108584.

El-Temsah, Y. S., Sevcu, A., Bobčíková, K., Černík, M., Joner, E. J., 2016: DDT Degradation Efficiency and Ecotoxicological Effects of Two Types of Nano-Sized Zero-Valent Iron (nZVI) in Water and Soil. *Chemosphere*, volume 144: 2221-2228. https://doi.org/10.1016/j.chemosphere.2015.10.122.

Fajardo, C., Gil-Díaz, M. M., Costa, G., Alonso, J., Guerrero, A. M., Nande, M., Lobo, M. C., Martín, M., 2015: Residual Impact of Aged nZVI on Heavy Metal-Polluted Soils. *Science of the Total Environment*, volume 535: 79-84. https://doi.org/10.1016/j.scitotenv.2015.03.067.

Fan, D., Anitori, R. P., Tebo, B. M., Tratnyek, P. G., Lezama Pacheco, J. S., Kukkadapu, R. K., Engelhard, M. H., Bowden, M. E., Kovarik, L., Arey, B. W., 2013: Reductive Sequestration of Pertechnetate ($^{99}TcO_4^-$) by Nano Zero-Valent Iron (nZVI) Transformed by Abiotic Sulfide. *Environmental Science & Technology*, volume 47, issue 10: 5302–5310. https://doi.org/10.1021/es304829z.

Garcia, A. N., Zhang, Y., Ghoshal, S., He, F., O´Carroll, D. M., 2021: Recent Advances in Sulphidated Zerovalent Iron for Contaminant Transformation. *Environmental Science & Technology*, volume 55, issue 13: 8464-8483. https://doi.org/10.1021/acs.est.1c01251.

Ghosh, I., Mukherjee, A., Mukherjee, A., 2017: *In Planta* Genotoxicity of nZVI: Influence of Colloidal Stability on Uptake, DNA Damage, Oxidative Stress and Cell Death. *Mutagenesis*, volume 32, issue 3: 371–387. https://doi.org/10.1093/mutage/gex006.

Gil-Díaz, M. M., Álvarez, M. A., Alonso, J., Lobo, M. C., 2020: Effectiveness of Nanoscale Zero-Valent Iron for the Immobilization of Cu and/or Ni in Water and Soil Samples. *Scientific Reports*, volume 10: 15927. https://doi.org/10.1038/s41598-020-73144-7.

Gil-Díaz, M. M., Álvarez-Aparicio, J., Alonso, J., Mancho, C., Lobo, M. C., González, J., García-Gonzalo, P., 2024: Soil Properties Determine the Impact of nZVI on *Lactuca sativa* L and its Rhizosphere. *Environmental Pollution*, volume 345: 122683. https://doi.org/10.1016/j.envpol.2023.122683.

Gou, N., Onnis-Hayen, A., Gu, A. Z., 2010: Mechanistic Toxicity Assessment of Nanomaterials by Whole-Cell-Array Stress Genes Expression Analysis. *Environmental Science & Technology*, volume 44, issue 15: 5964-5970. https://doi.org/10.1021/es100679f.

Grieger, K. D., Fjordbøge, A., Hartmann, N. B., Eriksson, E., Bjerg, P. L., Baun, A., 2010: Environmental Benefits and Risks of Zero-Valent Iron Nanoparticles (nZVI) for in situ Remediation: Risk Mitigation or Trade-Off? *Journal of Contaminant Hydrology*, volume 118, issue 3 & 4: 165–183. https://doi.org/10.1016/j.jconhyd.2010.07.011.

Guha, T., Mukherjee, A., Kundu, R., 2022: Nano-Scale Zero Valent Iron (nZVI) Priming Enhances Yield, Alters Mineral Distribution and Grain Nutrient Content of *Oryza sativa* L. cv. Gobindobhog: A Field Study. *Journal of Plant Growth Reguation*, volume 41: 710-733. https://doi.org/10.1007/s00344-021-10335-0.

Guo, Y., Li, X., Liang, L., Lin, Z., Su, X., Zhang, W., 2021: Immobilization of Cd in Contaminated Soils Using Sulphidated Nanoscale Zero-Valent Iron:

Effectiveness and Remediation Mechanism. *Journal of Hazardous Materials*, volume 420: 126605. https://doi.org/10.1016/j.jhazmat.2021.126605.

Han, Z., Salawu, O. A., Zenobio, J. E., Zhao, Y., Adeleye, A. S., 2021: Emerging Investigator Series: Immobilization of As in Soil by Nanoscale Zerovalent Iron: Role of Sulphidation and Application of Machine Learning. *Environmental Science: Nano*, volume 8: 619-633. https://doi.org/10.1039/d0en01202e.

Hoch, L. B., Mack, E. J., Hydutsky, B. W., Hershman, J. M., Skluzacek, J. M., Mallouk, T. E., 2008: Carbothermal Synthesis of Carbon-supported Nanoscale Zero-valent Iron Particles for the Remediation of Cr(VI). *Environmental Science & Technology*, volume 42, issue 7: 2600-2605. https://doi.org/10.1021/es702589u.

Hong, Y. K., Kim, J. W., Lee, S. P., Yang, J. E., Kim, S. C., 2022: Effect of Combined Soil Amendment on Immobilization of Bioavailable As and Pb in Paddy Soil. *Toxics*, volume 10, issue 2: 90. https://doi.org/10.3390/toxics10020090.

Huang, D., Yang, Y., Deng, R., Gong, X., Zhou, W., Chen, S., Li, B., Wang, G., 2021: Remediation of Cd -Contaminated Soil by Modified Nanoscale Zero-Valent Iron: Role of Plant Root Exudates and Inner Mechanisms. *International Journal of Environmental Research and Public Health*, volume 18, issue 11: 5887. https://doi.org/10.3390/ijerph18115887.

Huot, H., Simonnot, M., Watteau, F., Marion, P., Yvon, J., Donato, P.D., Morel, J. L., 2014: Early Transformation and Transfer Processes in a Technosol Developing on Iron Industry Deposits. *European Journal of Soil Science*, volume 65, issue 4: 470-484. https://doi.org/10.1111/ejss.12106.

Jamei, M. R., Khosravi, M. R., Anvaripour, B., 2013: Investigation of Ultrasonic Effect on Synthesis of Nano Zero Valent Iron Particles and Comparison with Conventional Method. *Asia-Pacific Journal of Chemical Engineering*, volume 8, issue 5: 767-774. https://doi.org/10.1002/apj.1720.

Jiang, D., Hu, X., Wang, R., Yin, D., 2015: Oxidation of Nanoscale Zero-Valent Iron Under Sufficient and Limited Dissolved Oxygen: Influences on Aggregation

Behaviours. *Chemosphere*, volume 122: 8-13. https://doi.org/10.1016/j.chemosphere.2014.09.095.

Jiang, D., Zeng, G., Huang, D., Chen, M., Zhang, C., Huang, C., Wan, J., 2018: Remediation of Contaminated Soils by Enhanced Nanoscale Iron. *Environmental Research*, volume 163: 217-227. https://doi.org/10.1016/j.envres.2018.01.030.

Jiang, M., Chen, R., Cao, B., Wang, F., 2023: The Performance of Temperature and Acid-Modified Sludge in Removing Lead and Cd . *Environmental Science and Pollution Research*, volume 30: 76072-76084. https://doi.org/10.1007/s11356-023-27741-4.

Johan, P. D., Ahmed, O. H., Omar, L., Hasbullah, N. A., 2010: Phosphorus Transformation in Soils Following Co-Application of Charcoal and Wood Ash. *Agronomy*, volume 11, issue 10. https://doi.org/10.3390/agronomy11102010.

Johnson, R. L., Johnson, G. O., Nurmi, J. T., Tratnyek, P. G., 2009: Natural Organic Matter Enhanced Mobility of Nano Zerovalent Iron. *Environmental Science & Technology*, volume 43, issue 14: 5455-5460. https://doi.org/10.1021/es900474f.

Kadu, B. S. & Chikate, R. C., 2013: nZVI Based Nanocomposites: Role of Noble Metal and Clay Support on Chemisorptive Removal of Cr(VI). Journal of Environmental Chemical Engineering, volume 1, issue 3: 320-327. https://doi.org/10.1016/j.jece.2013.05.011.

Kanel, S. R., Manning, B., Charlet, L., Choi, H., 2005: Removal of As(III) from Groundwater by Nanoscale Zero-Valent Iron. *Environmental Science & Technology*, volume 39, issue 5: 1291-1298. https://doi.org/10.1021/es048991u.

Ken, D. S. & Sinha, A., 2020: Recent Developments in Surface Modification of Nano Zero-Valent Iron (nZVI): Remediation, Toxicity and Environmental Impacts. *Environmental Nanotechnology, Monitoring, and Management*, volume 14: 100344. https://doi.org/10.1016/j.enmm.2020.100344.

Kheskwani, U, & Ahammed, M. M., 2023: Removal of Water Pollutants Using Plant-Based Nanoscale Zero-Valent Iron: A Review. *Water Science and Technology*, volume 88, issue 5: 1207–1231. https://doi.org/10.2166/wst.2023.270.

Kim, J. H., Kim, D., Seo, S. M., Kim, D., 2019: Physiological Effects of Zero-Valent Iron Nanoparticles in Rhizosphere on Edible Crop, *Medicago sativa* (Alfalfa), Grown in Soil. *Ecotoxicology*, volume 28: 869-877. https://doi.org/10.1007/s10646-019-02083-5.

Kommana, G., Grüneberg, B., Hupfer, M., 2023: Iron from Lignite Mining Increases Phosphorus Fixation in Sediments, but Does Not Affect Trophic States of Lakes Along River Spree (Germany). *Water, Air, & Soil Pollution*, volume 234: 454. https://doi.org/10.1007/s11270-023-06441-2.

Krol, M. M., Oleniuk, A. J., Kocur, C. M., Sleep, B. E., Bennett, P., Xiong, Z., O´Carroll, D. M., 2013: A Field-Validated Model for in situ Transport of Polymer-Stabilized nZVI and Implications for Subsurface Injection. *Environmental Science & Technology*, volume 47, issue 13: 7332–7340. https://doi.org/10.1021/es3041412.

Latif, A., Sheng, D., Sun, K., Si, Y., Azeem, M., Abbas, A., Bilal, M., 2020: Remediation of Heavy Metals Polluted Environment Using Fe-Based Nanoparticles: Mechanisms, Influencing Factors, And Environmental Implications. *Environmental Pollution*, volume 264: 114728. https://doi.org/10.1016/j.envpol.2020.114728.

Lee, C., Kim, J. Y., Lee, W. I., Nelson, K. L., Yoon, J., Sedlak, D. L., 2008: Bactericidal Effect of Zero-Valent Iron Nanoparticles on Escherichia Coli. *Environmental Science & Technology*, volume 42, issue 13: 4927–4933. https://doi.org/10.1021/es800408u.

Li, K., Li, J., Qin, F., Dong, H., Wang, W., Luo, H., Qin, D., Zhang, C., Tan, H., 2023: Nano Zero Valent Iron in the 21st Century: A Data-Driven Visualization and Analysis of Research Topics And Trends. *Journal of Cleaner Production*, volume 415: 137812. https://doi.org/10.1016/j.jclepro.2023.137812.

Li, M. & Luo, L., 2020: Review on Application of Nanomaterials in Soil Remediation. *Journal of Physics: Conference Series*, volume 1637: 012070. https://doi.org/10.1088/1742-6596/1637/1/012070.

Li, M., Zhang, P., Adeel, M., Guo, Z., Chetwynd, A. J., Ma, C., Bai, T., Hao, Y., Rui, Y., 2021a: Physiological Impacts of Zero Valent Iron, Fe_3O_4 and Fe_2O_3 Nanoparticles in Rice Plants and Their Potential as Fe Fertilizers. *Environmental Pollution*, volume 269: 116134. https://doi.org/10.1016/j.envpol.2020.116134.

Li, Q., Chen, Z., Wang, H., Yang, H., Wen, T., Wang, S., Hu, B., Wang, X., 2021b: Removal of Organic Compounds by Nanoscale Zero-Valent Iron and its Composites. *Science of the Total Environment*, volume 792: 148546. https://doi.org/10.1016/j.scitotenv.2021.148546.

Li, S., Yan, W., Zhang, W. X., 2009: Solvent-Free Production of Nanoscale Zero-valent Iron (nZVI) with Precision Milling. *Green Chemistry*, issue 11: 1618-1626. https://doi.org/10.1039/B913056J.

Li, Y., Zhao, H., Zhu, L., 2021c: Remediation of Soil Contaminated with Organic Compounds by Nanoscale Zero-Valent Iron: A review. *Science of The Total Environment*, volume 760: 143413. https://doi.org/10.1016/j.scitotenv.2020.143413.

Li, Z., Lowry, G. V., Fan, J., Liu, F., Chen, J., 2018: High Molecular Weight Components of Natural Organic Matter Preferentially Adsorb onto Nanoscale Zero Valent Iron and Magnetite. *Science of the Total Environment*, volumes 628-629: 177-185. https://doi.org/10.1016/j.scitotenv.2018.02.038.

Liang, B., Xie, Y., Fang, Z., Tsang, E. P., 2014: Assessment of the Transport of Polyvinylpyrrolidone-Stabilised Zero-Valent Iron Nanoparticles in a Silica Sand Medium. *Journal of Nanoparticle Research*, volume 16: 2485. https://doi.org/10.1007/S11051-014-2485-0.

Ling, L., Huang, X. Y., Li, M., Zhang, W. X., 2017: Mapping the Reactions in a Single Zero-Valent Iron Nanoparticle. *Environmental Science & Technology*, volume 51, issue 24: 14293-14300. https://doi.org/10.1021/acs.est.7b02233.

Liu, F., Zhou, W. H., Yi, S., Geng, X., 2019: Morphological and Mineral Features of nZVI Induced Precipitation on Quartz Particles. *Environmental Geotechnics*, volume 8, issue 5: 357-364. https://doi.org/10.1680/jenge.18.00081.

Liu, N., Zhang, Y., Zheng, C., Tang, C., Guan, J., Guo, Y., 2023: Sulphidated Nanoscale Zero Valent Iron For In Situ Immobilization Of Cr(VI) In Soil And Response Of Indigenous Microbes. *Chemosphere*, volume 344: 140343. https://doi.org/10.1016/j.chemosphere.2023.140343.

Liu, Y., Majetich, S. A., Tilton, R. D., Sholl, D. S., Lowry, G. V., 2005: TCE Dechlorination Rates, Pathways, and Efficiency of Nanoscale Iron Particles with Different Properties. *Environmental Science & Technology*, volume 39, issue 5: 1338–1345. https://doi.org/10.1021/es049195r.

Ma, X. & Yan, J., 2018: Plant Uptake and Accumulation of Engineered Metallic Nanoparticles from Lab to Field Conditions. *Current Opinion in Environmental Science & Health*, volume 6: 16-20. https://doi.org/10.1016/j.coesh.2018.07.008.

Ma, X., Gurung, A., Deng, Y., 2013: Phytotoxicity and Uptake of Nanoscale Zero-Valent Iron (nZVI) by Two Plant Species. *Science of the Total Environment*, volume 443: 844-849. https://doi.org/10.1016/j.scitotenv.2012.11.073.

MacKenzie, K. & Georgi, A., 2019: nZVI Synthesis and Characterization. In: Phenrat, T. & Lowry, G. V. (eds.): Nanoscale Zerovalent Iron Particles for Environmental Restoration: From Fundamental Science to Field Scale Engineering Applications. Springer, New York: 45-95. https://doi.org/10.1007/978-3-319-95340-3.

Majid, N. M., Islam, M. M., Mathew, L., 2012: Heavy Metal Uptake and Translocation by Mangium (*Acacia mangium*) from Sewage Sludge Contaminated Soil. *Australian Journal of Crop Science*, volume 6, issue 8: 1228-1235. https://www.cropj.com/islam_6_8_2012_1228_1235.pdf.

Mao, L. & Ye, H., 2018: Influence of Redox Potential on Heavy Metal Behaviour in Soils: A Review. *The Research of Environmental Sciences*, volume 31, issue 10: 1669-1676. http://doi.org/10.13198/j.issn.1001-6929.2018.07.19.

Mielcarz-Skalska, L., Smolińska, B., Szynkowska-Jóźwik, M., 2021: Comparison of the Impact of Different Types of nZVI on *Lolium westerwoldicum*. *Agronomy*, volume 11, issue 3: 467. https://doi.org/10.3390/agronomy11030467.

Mishra, T., Pandey, V. C., 2019: Phytoremediation of Red Mud Deposits Through Natural Succession. In: Pandey, V. C. & Bauddh, K. (eds.): Phytomanagement of Polluted Sites: Market Opportunities in Sustainable Phytoremediation. Elsevier, Amsterdam: 409-424. https://doi.org/10.1016/B978-0-12-813912-7.00016-8.

Mitzia, A., Vítková, M., Komárek, M., 2020: Assessment of Biochar and/or Nano Zerovalent Iron for the Stabilisation of Zn, Pb and Cd : A Temporal Study of Solid-Phase Geochemistry Under Changing Soil Conditions. *Chemosphere*, volume 242: 125248. https://doi.org/10.1016/j.chemosphere.2019.125248.

Mokarram-Kashtiban, S., Hosseini, S. M., Kouchaksaraei, M. T., Younesi, H., 2019: The Impact of Nanoparticles Zero-Valent Iron (nZVI) and Rhizosphere Microorganisms on the Phytoremediation Ability of White Willow and its Response. *Environmental Science and Pollution Research*, volume 26: 10776-10789. https://doi.org/10.1007/s11356-019-04411-y.

Mokete, R., Eljamal, O., Sugihara, Y., 2020: Exploration of The Reactivity of Nanoscale Zero-Valent Iron (nZVI) Associated Nanoparticles in Diverse Experimental Conditions. *Chemical Engineering and Processing: Process Intensification*, volume 150: 107879. https://doi.org/10.1016/j.cep.2020.107879.

Monga, Y., Kumar, P., Sharma, R. K., Filip, J., Varma, R. S., Zbořil, R, Gawande, M. B., 2020: Sustainable Synthesis of Nanoscale Zerovalent Iron Particles for Environmental Remediation. *ChemSusChem*, volume 13: 3288 – 3305. https://doi.org/10.1002/cssc.202000290.

Mosquera-Losada, M. R., Muñoz, N., Rigueiro-Rodríguez, A., 2009: Agronomic Characterisation of Different Types of Sewage Sludge: Policy Implications. *Waste Management*, volume 30, issue 3: 492-503. http://doi.org/10.1016/j.wasman.2009.09.021.

Mu, Y., Jia, F., Ai, Z., Zhang, L., 2017: Iron Oxide Shell Mediated Environmental Remediation Properties of Nano Zero-Valent Iron. *Environmental Science: Nano*, volume 4: 27-45. https://doi.org/10.1039/C6EN00398B.

Muhammad, I., Puschenreiter, M., Wenzel, W. W., 2012: Cd and Zn Availability as Affected by pH Manipulation and its Assessment by Soil Extraction, DGT and

Indicator Plants. *Science of the Total Environment*, volume 416: 490-500. https://doi.org/10.1016/j.scitotenv.2011.11.029.

Nadagouda, M. N., Castle, A. B., Murdock, R. C., Hussain, S. M., Varma, R. S., 2010: In Vitro Biocompatibility of Nanoscale Zerovalent Iron Particles (nZVI) Synthesized Using Tea Polyphenols. *Green Chemistry*, volume 12: 114-122. https://doi.org/10.1039/B921203P.

Nirola, R., Megharaj, M., Palanisami, T., Aryal, R., Venkateswarlu, K., Naidu, R., 2015: Evaluation of Metal Uptake Factors of Native Trees Colonizing an Abandoned Copper Mine – A Quest for Phytostabilization. *Journal of Sustainable Mining*, volume 14, issue 3: 115-123. https://doi.org/10.1016/j.jsm.2015.11.001.

Nurmi, J. T., Tratnyek, P. G., Sarathy, V., Baer, D. R., Amonette, J. E., Pecher, K., Wang, C., Linehan, J. C., Matson, D. W., Penn, R. L., Driessen, M. D., 2005: Characterization and Properties of Metallic Iron Nanoparticles: Spectroscopy, Electrochemistry, and Kinetics. *Environmental Science & Technology*, volume 39, issue 5: 1221–1230. https://doi.org/10.1021/es049190u.

Ohshima, H., 2012: Electrical Phenomena at Interfaces and Biointerfaces: Fundamentals and Applications in Nano-, Bio-, And Environmental Sciences. Wiley, Hoboken, NJ, USA. 850 pp.

Pasinszki, T., & Krebsz, M., 2020: Synthesis and Application of Zero-Valent Iron Nanoparticles in Water Treatment, Environmental Remediation, Catalysis, and Their Biological Effects. *Nanomaterials*, volume 10, issue 5: 917. https://doi.org/10.3390/nano10050917.

Phenrat, T., Lowry, G. V., Babakhani, P., 2019: Nanoscale Zerovalent Iron (nZVI) for Environmental Decontamination: A Brief History of 20 Years of Research and Field-Scale Application. In: Phenrat, T. & Lowry, G. V. (eds.): Nanoscale Zerovalent Iron Particles for Environmental Restoration: From Fundamental Science to Field Scale Engineering Applications. Springer, New York: 1-43. https://doi.org/10.1007/978-3-319-95340-3.

Phenrat, T., Kim, H. J., Fagerlund, F., Illangasekare, T., Tilton, R. D., Lowry, G. V., 2009a: Particle Size Distribution, Concentration, and Magnetic Attraction Affect Transport of Polymer-Modified Fe0 Nanoparticles in Sand Columns:

Environmental Science & Technology, volume 43, issue 13: 5079-5085. https://doi.org/10.1021/es900171v.

Phenrat, T., Long, T. C., Lowry, G. V., Veronesi, B., 2009b: Partial Oxidation ("("Aging") and Surface Modification Decrease the Toxicity of Nanosized Zerovalent Iron. *Environmental Science & Technology*, volume 43: 195–200. https://doi.org/10.1021/es801955n.

Phenrat, T., Kim, H. J., Fagerlund, F., Illangasekare, T., Lowry, G. V., 2010: Empirical Correlations to Estimate Agglomerate Size and Deposition During Injection of a Polyelectrolyte-Modified Fe0 Nanoparticle at High Particle Concentration in Saturated Sand. *Journal of Contaminant Hydrology*, volume 118, issues 3 & 4: 152–164. https://doi.org/10.1016/j.jconhyd.2010.09.002.

Phenrat, T., Saleh, N., Sirk, K., Tilton, R. D., Lowry, G. V., 2007: Aggregation and Sedimentation of Aqueous Nanoscale Zerovalent Iron Dispersions. *Environmental Science & Technology*, volume 41: 284–290. https://doi.org/10.1021/es061349a.

Ramos, M. A. V., Yan, W., Li, X. Q., Koel, B. E., Zhang, W. X., 2009: Simultaneous Oxidation and Reduction of As by Zero-Valent Iron Nanoparticles: Understanding the Significance of the Core−Shell Structure. *The Journal of Physical Chemistry*, volume 113, issue 33: 14591-14594. https://doi.org/10.1021/jp9051837.

Saed-Moucheshi, A., Shekoofa, A., Pessarakli, M., 2011: Reactive Oxygen Species (ROS) Generation and Detoxifying in Plants. *Journal of Plant Nutrition*, volume 37, issue 10: 1573-1585. https://doi.org/10.1080/01904167.2013.868483.

Saleh, N., Kim, H. J., Phenrat, T., Matyjaszewski, K., Tilton, R. D., Lowry, G. V., 2008: Ionic Strength and Composition Affect the Mobility of Surface-Modified Fe0 Nanoparticles in Water-Saturated Sand Columns. *Environmental Science & Technology*, volume 42, issue 9: 3349–3355. https://doi.org/10.1021/es071936b.

Sastry, M., Ahmad, A., Khan, M. I., Kumar, R., 2003: Biosynthesis of Metal Nanoparticles Using Fungi and Actinomycete. *Current Science*, volume 85, issue 2: 162-170. https://www.jstor.org/stable/24108579.

Schrick, B., Hydutsky, B. W., Blough, J. L., Mallouk, T. E., 2004: Delivery Vehicles for Zerovalent Metal Nanoparticles in Soil and Groundwater. Chemistry of Materials, volume 16, issue 11: 2187–2193. https://doi.org/10.1021/cm0218108.

Sebastian, A. & Prasad, M. N. V., 2018: Exogenous Citrate and Malate Alleviate Cd Stress in *Oryza sativa* L.: Probing Role of Cd Localization and Iron Nutrition. *Ecotoxicology and Environmental Safety*, volume 166: 215-222. https://doi.org/10.1016/j.ecoenv.2018.09.084.

Sharma, D., Kanchi, S., Bisetty, K., 2019: Biogenic Synthesis of Nanoparticles: A Review. *Arabian Journal of Chemistry*, volume 12, issue 8: 3576-3600. https://doi.org/10.1016/j.arabjc.2015.11.002.

Stefaniuk, M., & Oleszczuk, P., 2016: Review on Nano Zerovalent Iron (nZVI): From Synthesis to Environmental Applications. *Chemical Engineering Journal*, volume 287: 618-632. https://doi.org/10.1016/j.cej.2015.11.046.

Su, Y., Lowry, G. V., Jassby, D., Zhang, Y., 2019: Sulfide-Modified nZVI (S-nZVI): Synthesis, Characterization, and Reactivity. In: Phenrat, T. & Lowry, G. V. (eds.): Nanoscale Zerovalent Iron Particles for Environmental Restoration: From Fundamental Science to Field Scale Engineering Applications. Springer, New York: 359-386. https://doi.org/10.1007/978-3-319-95340-3.

Sun, Y., Jing, R., Zheng, F., Zhang, S., Jiao, W., Wang, F., 2019: Evaluating Phytotoxicity of Bare and Starch-Stabilized Zero-Valent Iron Nanoparticles in Mung Bean. *Chemosphere*, volume 236: 124336. https://doi.org/10.1016/j.chemosphere.2019.07.067.

Taghavy, A., Costanza, J., Pennell, K. D., Abrio, L. M., 2010: Effectiveness of Nanoscale Zero-Valent Iron for Treatment of a PCE–DNAPL Source Zone. *Journal of Contaminant Hydrology*, volume 118, issues 3 & 4: 128–142. https://doi.org/10.1016/j.jconhyd.2010.09.001.

Tarekegn, M. M., Hiruy, A. M., Dekebo, A. H., 2021: Nano Zero Valent Iron (nZVI) Particles for the Removal of Heavy Metals (Cd $^{2+}$, Cu^{2+} and Pb^{2+}) from Aqueous Solutions. *RSC Advances*, volume 11, issue 30: 18539–18551. https://doi.org/10.1039%2Fd1ra01427g.

Teodoro, M., Clemente, R., Ferrer-Bustins, E., Martínez-Fernández, D., Bernal, M. P., Vitková, M., Vítek, P., Komárek, M., 2020: Nanoscale Zero-Valent Iron Has Minimum Toxicological Risk on the Germination and Early Growth of Two Grass Species with Potential for Phytostabilization. *Nanomaterials*, volume 10, issue 8: 1537. https://doi.org/10.3390%2Fnano10081537.

Tessier, A., Campbell, P. G. C., Bisson, M., 1979: Sequential Extraction Procedure for The Speciation of Particulate Trace Metals. *Analytical Chemistry*, volume 51, issue 7: 844–851. https://doi.org/10.1021/ac50043a017.

Thakkar, K. N., Mhatre, S. S., Parikh, R. Y., 2010: Biological Synthesis of Metallic Nanoparticles. *Nanomedicine: Nanotechnology, Biology, and Medicine*, volume 6, issue 2: 275-262. https://doi.org/10.1016/j.nano.2009.07.002.

Tolaymat, T., Genaidy, A., Abdelraheem, W., Dionysiou, D., Andersen, C., 2017: The Effects of Metallic Engineered Nanoparticles Upon Plant Systems: An Analytic Examination of Scientific Evidence. *Science of The Total Environment*, volume 579: 93-106. https://doi.org/10.1016/j.scitotenv.2016.10.229.

Truter, W. F., Rethman, N. F. G., Reynolds, K. A., Kruger, R. A., 2001: The Use of a Soil Ameliorant based on Fly ash and Sewage Sludge. *International Ash Utilization Symposium*: 80. https://p2infohouse.org/ref/45/44800.pdf.

Valiev, R. Z., 2000: Bulk Nanostructured Materials from Severe Plastic Deformation. *Progress in Materials Science*, volume 45, issue 2: 103-189. https://doi.org/10.1016/S0079-6425(99)00007-9.

Wang, C. B. & Zhang, W. X., 1997: Synthesizing Nanoscale Iron Particles for Rapid and Complete Dechlorination of TCE and PCBs. *Environmental Science & Technology*, volume 31, issue 7: 2154-2156. https://doi.org/10.1021/es970039c.

Wang, J., Fang, Z., Cheng, W., Yan, X., Tsang, P. E., Zhao, D., 2016: Higher Concentrations of Nanoscale Zero-Valent Iron (nZVI) in Soil Induced Rice Chlorosis Due to Inhibited Active Iron Transportation. *Environmental Pollution*, volume 210: 338-345. https://doi.org/10.1016/j.envpol.2016.01.028.

Wang, Y. & Lin, D., 2017: The Interaction Between Nano Zero-Valent Iron and Soil Components and Its Environmental Implication. *Progress in Chemistry*, volume 29, issue 9: 1072-1081. https://doi.org/10.7536/PC170526.

Wang, Y., Liu, Y., Yang, K., Lin, D., 2020: Reciprocal Interference of Clay Minerals and Nanoparticulate Zero-Valent Iron on Their Interfacial Interaction with Dissolved Organic Matter. *Science of The Total Environment*, volume 739: 140372. https://doi.org/10.1016/j.scitotenv.2020.140372.

Wang, Y., Liu, Y., Su, G., Yang, K., Lin, D., 2021a: Transformation and Implication of Nanoparticulate Zero Valent Iron in Soils. *Journal of Hazardous Materials*, volume 412: 125207. https://doi.org/10.1016/j.jhazmat.2021.125207.

Wang, Y., Chen, S., Deng, C., Shi, X., Cota-Ruiz, K., White, J. C., Zhao, L., Gardea-Torresdey, J. L., 2021b: Metabolomic Analysis Reveals Dose-Dependent Alteration of Maize (*Zea mays* L.) Metabolites and Mineral Nutrient Profiles Upon Exposure to Zerovalent Iron Nanoparticles. *NanoImpact*, volume 23: 100336. https://doi.org/10.1016/j.impact.2021.100336.

Wojcieszek, J., Chay, S., Jiménez-Lamana, J., Curie, C., Mari, S., 2023: Study of the Stability, Uptake and Transformations of Zero Valent Iron Nanoparticles in a Model Plant by Means of an Optimised Single Particle ICP-MS/MS Method. *Nanomaterials*, volume 13, issue 11: 1736. https://doi.org/10.3390/nano13111736.

Xie, Y. & Cwiertny, D. M., 2010: Use of Dithionite to Extend the Reactive Lifetime of Nanoscale Zero-Valent Iron Treatment Systems. *Environmental Science & Technology*, volume 44, issue 22: 8649-8655. https://doi.org/10.1021/es102451t

Xiu, Z. M., Jin, Z. H., Li, T. L., Mahendra, S., Lowry, G. V., Alvarez, P. J., 2010: Effects of Nano-Scale Zero-Valent Iron Particles on a Mixed Culture Dechlorinating Trichloroethylene. *Bioresource Technology*, volume 101, issue 4: 1141–1146. https://doi.org/10.1016/j.biortech.2009.09.057.

Yaacob, W. Z., Kamaruzaman, N., Samsudin, A. R., 2012: Development of Nano-Zero Valent Iron for the Remediation of Contaminated Water. *Chemical*

Engineering Transactions, volume 28: 25-30. https://doi.org/10.3303/CET1228005.

Yang, G. C. C., Tu, H. C., Hung, C. H., 2007: Stability of Nanoiron Slurries and Their Transport in the Subsurface Environment. *Seperation and Purification Technology*, volume 58, issue 1: 166-172. https://doi.org/10.1016/j.seppur.2007.07.018.

Yang, S., Liu, A., Liu, J., Liu, Z., Zhang, W., 2022: Advance of Sulphidated Nanoscale Zero-Valent Iron: Synthesis, Properties and Environmental Application. *Acta Chimica Sinica*, volume 80, issue 11: 1536-1554. https://doi.org/10.6023/A22080345.

Ye, J., Luo, Y., Sun, J., Shi, J., 2021: Nanoscale Zero-Valent Iron Modified by Bentonite with Enhanced Cr(VI) Removal Efficiency, Improved Mobility, and Reduced Toxicity. *Nanomaterials*, volume 11, issue 10: 2850. https://doi.org/10.3390/nano11102580.

Yoon, H., Kang, Y. G., Chang, Y. S., Kim, J. H., 2019: Effects of Zerovalent Iron Nanoparticles on Photosynthesis and Biochemical Adaptation of Soil-Grown *Arabidopsis thaliana*. *Nanomaterials*, volume 9, issue 11: 1543. https://doi.org/10.3390%2Fnano9111543.

Yusuf, E. O., Amber, I., Officer, S., Oluyemi, G. F., 2024: Transport of Nanoparticles in Porous Media and Associated Environmental Impact: A Review. *Journal of Engineering Research*. https://doi.org/10.1016/j.jer.2024.01.006.

Zand, A. D. & Tabrizi, A. M., 2020: Effect of Zero-Valent Iron Nanoparticles on the Phytoextraction Ability of Kochia Scoparia and its Response in Pb Contaminated Soil. *Environmental Engineering Research*, volume 26, issue 4: 200227. https://doi.org/10.4491/eer.2020.227.

Zandi, P. & Schnug, E., 2022: Reactive Oxygen Species, Antioxidant Responses and Implications from a Microbial Modulation Perspective. *Biology*, volume 11, issue 2: 155. https://doi.org/10.3390%2Fbiology11020155.

Zhang, M., Dong, Y., Gao, S., Cai, P., Dong, J., 2019a: Effective Stabilization and Distribution of Emulsified Nanoscale Zero-Valent Iron by Xanthan for

Enhanced Nitrobenzene Removal. *Chemosphere*, volume 223: 375-382. https://doi.org/10.1016/j.chemosphere.2019.02.099.

Zhang, S., Li, X., Yang, Y., Li, Y., Chen, J., Ding, F., 2019b: Adsorption, Transformation, and Colloid-Facilitated Transport of Nano-Zero-Valent Iron in Soils. *Environmental Pollutants and Bioavailability*, volume 31, issue 1: 208-218. https://doi.org/10.1080/26395940.2019.1608865.

Zhu, F., Li, L., Ren, W., Deng, X., Liu, D., 2017: Effect of pH, Temperature, Humic Acid and Coexisting Anions on Reduction of Cr(VI) In The Soil Leachate By nZVI/Ni Bimetal Material. *Environmental Pollution*, volume 227: 444-450. https://doi.org/10.1016/j.envpol.2017.04.074.

Zinzala, V. J., Naik, J. R., Tripathi, S., Patel, K. G., Singh, N., 2023: Comparison of Different Digestion Methods for Analysis of Multi Element (P, K, Fe, Mn, Zn and Cu) from Plant. *The Pharma Innovation Journal*, volume 12, issue 3: 3122-3129. https://www.thepharmajournal.com/archives/2023/vol12issue3/PartAG/12-3-444-623.pdf.

Legislative Sources

Decree No. 437/2016 Coll., on the conditions of use of treated sludge on agricultural land, as amended.

Internet Sources

Nano Iron, s.r.o, ©2010: NANOFER 25DS (on-line) [cit. 2023. 10. 20], available at <https://nanoiron.cz/en/products/zero-valent-iron-nanoparticles/nanofer-25ds>.

NanoRem: Home (on-line) [cit. 2023. 09. 25], available at <https://www.nanorem.eu/index.aspx>.